AD-A038 152 PENNSYLVANIA STATE UNIV UNIVERSITY PARK MATERIALS RE--ETC F/G 9/1
CERAMIC PIEZOELECTRIC TRANSDUCERS.(U)
JAN 77 L E CROSS, J V BIGGERS, R E NEWNHAM N00014-76-C-0515

UNCLASSIFIED NL

1 OF 1
AD
A038152

END
DATE
FILMED
4-77

See 1473

12

CERAMIC PIEZOELECTRIC TRANSDUCERS

Annual Summary Report
to the
Office of Naval Research
Arlington, Virginia 22217

Contract No. N00014-76-C-0515

January 1977

L. E. Cross
J. V. Biggers
R. E. Newnham

THE MATERIALS RESEARCH LABORATORY

THE PENNSYLVANIA STATE UNIVERSITY

UNIVERSITY PARK, PENNSYLVANIA

Table of Contents

ABSTRACT

This reports documents progress in the first year of a comprehensive program to develop new and improved materials for ceramic piezoelectric transducers. For many years, formulations in the $PbZrO_3$:$PbTiO_3$ (PZT) family of ferroelectric solid solutions, with compositions chosen to be close to the morphotropic rhombohedral: tetragonal ferroelectric phase transition have been very widely used for transducers.

For these conventional PZT type ceramics this program seeks to clarify the roles of the different deformation mechanisms in both 'hard' and 'soft' formulations, and to clearly delineate the influence of the ceramic microstructure in modifying the 'averaged' single crystal properties of the constituent crystallites. These studies include a careful intercomparison of the microstructure, chemical microhomogeneity and physical properties of samples with precisely controlled initial chemistry, fabricated by a wide range of different ceramic techniques. To aid in the separation of single crystal 'single domain' properties, a phenomenological Elastic Gibbs function to describe PZTs with compositions close to the morphotropic boundary is being developed, and ADAGE computer graphic methods are being developed to depict the full three-dimensional polarization surfaces near the stable phases so that the role of internal stresses and electric fields can be quantitatively analyzed.

To attempt more radical advance in polycrystal materials three different approaches are being taken:

(1) To broaden the composition base for transducers fabricated by traditional methods, we seek new ferroelectric compounds with high Curie temperature and high effective prototypic symmetry. Tellurium containing compounds with perovskite structure in the family Sr_2CdTeO_6 which have been reported to have ferroic transition temperatures up to 960°C are being studied. In the less symmetric $Sr_2Nb_2O_7$ and $Nd_2Ti_2O_7$ pyrochlore derivative structures very high Curie temperature up to 1650°C have been reported. Techniques are being developed to produce glass or microcrystalline materials in these families, seeking "glass-like" ferroelectric properties and materials which would be polable in any orientation.

(2) To break the original boundary condition of macroscopic homogeneity deliberate composition gradients are being introduced by co-firing stacked layers of tape cast thin sections with suitably controlled composition. Preliminary studies show that both ferroelectric and antiferroelectric formulations can be co-fired, promising a range of control of both electrical poling and elastic stress distribution in these structures.

(3) To eliminate the need for exceedingly high prototype symmetry, grain oriented ceramics are being developed as a potential "hybrid" between single crystal and ceramic forms. Initial work is concentrated on the family of bismuth oxide layer structure ferroelectrics where the platy morphology of the micro-crystals allows the use of many simple ceramic techniques for generating oriented microstructures.

A new type of device is under study which makes the use of a multilayer monolithic structure with integrated electrodes to generate large electrostrictive deformations at low applied voltages in an unpoled high K dielectric. These elements show considerable promise for displacement transducers in adaptive optics and as controllable generators for acoustic holography.

1. INTRODUCTION

Ceramic piezoelectric transducers are important components of many vital military electronic systems. Uses range from the very large high-power low-frequency elements of Naval Sonar Systems to the very small high-frequency transducers used in ultrasonic flaw detection and other types of NDT. Piezoelectric resonant devices are widely used for frequency control and filtering, and the possibilities of new device structures using traveling bulk and surface waves present challenging new problems for the design of more efficient piezoelectric materials.

In the rapidly developing area of Adaptive Optics, new needs for piezoelectrically activated displacement transducers for optical path length control, and for high density integrated electrode systems in multi-dither mirror configurations provide goals which are at the limits of capability for the present generation of transducer materials.

For biomedical applications there are urgent needs for better higher frequency transducers which have good acoustic matching to water, and particularly for miniature elements which may be simply fabricated into transducer arrays both for projection and reception in acoustic diagnostic imaging.

Heretofore, polycrystalline piezoelectric transducers have been fabricated almost exclusively from macroscopically homogeneous solid solutions of ferroelectric compounds, cold pressed and sintered to a dense polycrystal microstructure with random arrangement of crystal axes between the individual constituent crystallites. The need to electrically pole the polycrystal leads, under these circumstances to the choice of ferroelectric compounds with high prototype symmetry in the paraelectric phase, and thus with many different orientations available for the spontaneous electric polarization in the domain structure of the ferroelectric phase. For many years, formulations in the $PbZrO_3$:$PbTiO_3$ (PZT) family of solid solutions, with compositions chosen so as to be close to the morphotropic rhombohedral:tetragonal ferroelectric phase boundary, have been widely used in transducer applications.

Through very extensive painstaking studies of compositions modified by minor (less than 5 wt%) additions of aliovalent metal cations, usually added

as oxides, the major manufacturers have formulated empirical 'rules' of how to modify, and in part control the ferroelectric properties in these complex ceramics. In this manner, formulations have been developed which have high coupling coefficients (K_{33} up to 0.75) high dielectric constants ($\varepsilon_{33} \sim 3{,}500$) and reasonable stability. Unfortunately, with many of the compositional studies which have been performed, the exact nature of the distribution of the added components have not been ascertained. The degree of micro-homogeneity grain to grain, and between grain and grain boundary region has not been delineated and the exact role of the modifier ions in changing single crystal, as distinct from ceramic microstructure related properties, remains obscure.

Theoretically, it is clear that the basic electroelastic coupling in all the piezoelectric ceramics resides in the electrostrictive effect in the prototype (paraelectric structure). In the ferroelectric phase, however, this can give rise to three rather different contributions to dimension change under field.

(1) The spontaneous polarization biased electrostriction of the ferroelectric single domain state gives the total single domain piezoelectric response. Ferroelectric domain switching through 180° will modify this effect, by changing the sign of all piezoelectric terms in the matrix of single domain properties. However, it will not of itself induce additional deformation since the spontaneous strain is strictive and thus does not depend on the sign of P_s.

(2) Ferroelastic-ferroelectric domain switching occurs when the spontaneous polarization reorients through angles other than 180°. The spontaneous electrostrictive deformation associated with the appearance of P_s will give rise to overall dimension changes (referred to any fixed set of axes) which differ in the two domains. The field-induced motion of walls separating such domains must therefore cause changes in crystal shape, i.e., such domain motion carries elastic strain and the switching process is ferroelastic as well as ferroelectric. Such wall motion could contribute both to the dielectric and piezoelectric properties in the crystal.

(3) Field induced ferroelectric phase changes are also possible in the PZT compositions used in transducer formulations, where the composition has been deliberately engineered to be close to a phase instability. It is possible for the applied electric field E to drive a ferroelectric-ferroelectric phase transition. Since the phase change involves both a change of magnitude and orientation of P_s in <u>all</u> domain states, the motion of a phase boundary under

field must carry strain and again must contribute to the elasto-electric character of the solid.

Clearly, the latter two mechanisms are of vital importance at the high field levels used in establishing the poled condition, however, the extent to which they contribute, if at all, to the very weak field 'linear' piezoelectric behavior in any particular composition is still an open question.

2. RATIONALE FOR TECHNICAL APPROACHES

The proposed technical approaches in this study are of two types: Evolutionary approaches seek to achieve a better understanding of the present family of PZT based materials and a consequent improvement of the present generation of transducer materials. In the revolutionary approaches some newer processing methods are utilized to break out of the constraints imposed by macroscopic homogeneity and random axial arrangement of the crystallites in the piezoceramic to produce strongly ferroelectric materials in polycrystal form for transducer applications.

2.1. Evolutionary Approaches

In the past, a great deal of emphasis has been placed upon the 'chemical' modification of PZT materials with compositions in Zr:Ti ratio chosen close to that required for morphotropy. Early work of this type undoubtedly contributed immensely to the development of present practical transducers, but further purely chemical modification in unlikely to lead to major improvements in the performance or in the basic understanding of these already complex systems.

It is our belief that a much more fruitful area of study is the interrelationship between ceramic microstructure, chemical micro-heterogeneity and the resulting physical properties. Such a study using modern preparation techniques to control the microstructure and heterogeneity, coupled with systematic characterization at each stage of processing, should give a range of samples from which a better separation of the intrinsic single crystal and ceramic microstructure related aspects of the material behavior can be achieved.

For such complex systems, no single technique or group of techniques can be definitive, and the preparation and characterization studies must be closely coupled to detailed dielectric, elastic and electro-elastic measurements on the same samples.

In parallel with the practical studies it is also desirable to approach the problem both theoretically and experimentally through the modeling of simpler more tractable systems which attempt to separate and assess the importance of the different individual electro-elastic coupling mechanisms.

The Devonshire phenomenological theory offers a simple approach to assess the effects of different elastic and electrical boundary conditions upon the single domain properties of any perovskite based ferroelectric. It would obviously be highly desirable to have Devonshire parameters to describe PZTs and a small effort is being focused onto this subject. Similarly in PLZT, where the optical transparency offers additional experimental parameters for the study of separation of intrinsic and domain related changes, measurements are being carried forward to determine the contribution to low field piezoelectricity associated with reversible ferroelastic-ferroelectric domain wall motion.

Discussions with several of the major engineering firms suggest that, in the displacement transducers for adaptive optics, the requirements differ significantly from those of other more conventional transducer functions. Powers available are limited but large linear displacements are required with minimum hysteresis and very low aging or deaging. In multi-dither configurations there is a need to integrate closely-spaced electrode arrangements within the body of the transducer. Present post poling techniques of mechanical fabrication are obviously expensive, time consuming and with limited potential for advance to the desired number of elements in the unit. Also, for present PZT materials the drive voltage requirements are embarrassingly large ($\sim$1,000 volts).

In materials like PZT which depend on a ferroelastic domain reorientation induced by a poling operation, aging and deaging at high field levels are unavoidable. However, in some of the newer high voltage capacitors which are based on perovskite compositions, hysteresis has been almost completely suppressed, aging rates can be extremely low, and at high field levels very sizeable elastic displacements can be induced by direct electrostriction. Techniques for integrating electrodes in multilayer configurations in these materials have been well worked out and a number of interesting and potentially useful configurations appear possible.

Our initial studies have been concerned with measuring the electrostriction parameters for a number of commercial and prototype dielectrics to select those materials with a high figure of merit for optical displacement transducer applications.

In the course of these studies we were made aware of the high efficiency of the simple electrostriction transducer based on a multilayer capacitor as a projector of ultrasound in water, and of an urgent need for transducer arrays

where the phase and amplitude of the transmitted signal could be controlled by an externally applied "influence function".

Since electrostriction is an essentially non-linear phenomenon, the possibility clearly exists for switching both amplitude and phase of a tuned transmitted signal by a D.C. bias applied to the element. Dielectric saturation normally 'linearizes' the electrostrictive effect (s_i vs E_i) at high field levels, however, in certain PLZTs where easy antiferroelectric:ferroelectric switching can occur, higher non-linearity can be deliberately induced. Such material appear to be attractive for medical ultrasonics and a small effort is being applied to these materials as a 'spin off' from the transducer work for adaptive optics.

2.2. Revolutionary Approaches

The approaches in this area are predicted upon the belief that the PZT family is close to the optimum which can be achieved for a macroscopically homogeneous randomly-axed polycrystal transducer. This belief is based upon the evidence in the literature that some 25 years of activity in ferroelectrics has not uncovered any more attractive alternative systems.

In these circumstances it appears desirable to seek relief from the original boundary conditions of macroscopic homogeneity with randomly oriented crystallites. Thus, we are examining techniques for producing deliberately tailored laminar heterogeneity and processing methods by which a preferred grain orientation can be introduced in the ceramic.

The objective in the first case is to make use of the control which laminar heterogeneity may afford to adjust the elastic and electrical boundary conditions at each interface to achieve better control of poling, depoling and aging phenomena. In the second case our objective is to eliminate the need for ferroelastic-ferroelectric switching to achieve effective poling. This would relieve the major incompatible dimension changes induced between grains during poling and thus the very strong internal stresses which are a major cause of aging. Also, with a very strongly preferred orientation, the need for many alternative polar orientations in the domain states is obviated, and the many families of strong ferroelectrics which stem from prototype phases of lower symmetry become interesting for polycrystal application.

3. PROGRESS REPORT

3.1. Processing Studies

3.1.1. Preparation of Powders

In keeping with the philosophy outlined in Section 2 above, our processing studies have been initiated using commercial formulations. Representative commercial compositions shown in Table 1, have been purchased and are being carefully characterized using:

(a) SEM particle size analysis,

(b) Surface area measurements,

(c) X-ray diffraction for phase identification,

(d) Optical emission spectroscopy for minor and trace element identification,

(e) Auger electron spectroscopy (AES) and Ion scattering spectroscopy for distribution of the major elements and 'impurities'.

In parallel with this work a similar characterization effort is being applied to several of the commercially used raw materials which are common to many of the proprietary formulations. In line with industrial experience, ZrO_2 has been selected as the component for most intensive study, and when this has been completed, PbO and TiO_2 will be similarly checked. In these raw material studies, special emphasis is being placed upon the computer controlled SEM technique for size and shape analysis together with our capabilities in AES and ISS to locate impurities and impurity gradients in the raw material powders.

A small effort is also being applied to the preparation of very pure chemically co-precipitated PZT compositions. Two specific processes are under study, one using soluble nitrates, and the other using acetate and butoxides. A PZT of composition $Pb(Ti_{0.48}Zr_{0.52})O_3$ has been prepared from lead acetate and titanium and zirconium tetra-n-butoxides. The as prepared powder has a very uniform particle size close to 0.5 μm and a surface area of 28 m^2/gm.

Table 1. PZT Formulations and Raw Materials

Prepared PZT Formulation

Type	Designation	Supplier
Navy I	401	Ultrasonics Powders, Inc.
Navy III	401 - 888	
Navy IV	501 A USH - 32	

Raw Materials for Study

Material	Grade	Supplier
PbO	Analyzed	J. T. Baker Chemical Co.
TiO_2 "	Analyzed Certified	J. T. Baker Chemical Co. Fisher Scientific Co.
ZrO_2	99.9%	TRW Electronics
SnO_2	99.9%	Alfa Products
TeO_2	99.5%	Alfa Products
Ta_2O_5	99.9%	Alfa Products
Nd_2O_3	Technical	Molycorporation
Nb_2O_5	99.5%	Alfa Products
La_2O_3	Purified	J. T. Baker Chemical Co.
$BaCO_3$	Certified	Fisher Scientific Co.
$CaCO_3$	Reagent	J. T. Baker Chemical Co.
$CdCO_3$	Reagent	Matheson Coleman Bell

Investigations of the kinetics of calcination using thermogravimetric (TGA) and differential thermal analysis (DTA) are now in progress.

3.1.2. Tape Casting

An essential pre-requisite for the development of the more sophisticated bodies with deliberate and controlled laminar heterogeneity, proposed in the more revolutionary approaches, is to establish the procedures for reliable tape casting of PZT formulations.

For initial study we have selected a commercial PZT powder (Ultrasonic Type 401) and a commercial binder system supplied by Cladan, Inc., which is widely used in tape casting perovskites for capacitor applications.

Parameters which are of importance in the tape casting process include:

(1) The viscosity of the slip as a function of the weight percent of PZT powder, and the manner in which this changes on changing particle size and shape in the ceramic component. Typical data for a powder milled for 48 hours at 300 RPM are given in Figure 1. It may be noted that at this size level, the viscosity does not begin to ascend rapidly until a weight fraction loading above 60 to 70%.

(2) Green (unfired) density of the tape as a function of weight fraction of PZT powder. Typical data for a similar powder to that used in the data of Figure 1 is shown in Figure 2. It may be noted that the green density, as expected, climbs steadily with increased loading up to the range of 60 to 70 wt%. Above this level, the curve flattens markedly due to the rise in viscosity leading to poor spreading.

(3) The kinetics of binder removal, which are essential to establish proper firing procedures which will avoid excessive outgasing, bubble formation and delamination in multilayer configurations. DTA and TGA methods have been used to establish the rates of binder removal both for the tape, and for a compatible commercial platinum electrode ink (Englehart E305A) which will be used in fabricating multilayer structures with integrated electrodes. Some of the DTA and TGA results are summarized in Figures 3 through 6.

Initial tape casting studies were carried through using a simple hand operated doctor blade on a small stationary glass plate. An automatic casting system is now under construction. This equipment will use a moving glass plate and an improved two blade hopper. It is designed to cast tapes up to 3 feet in

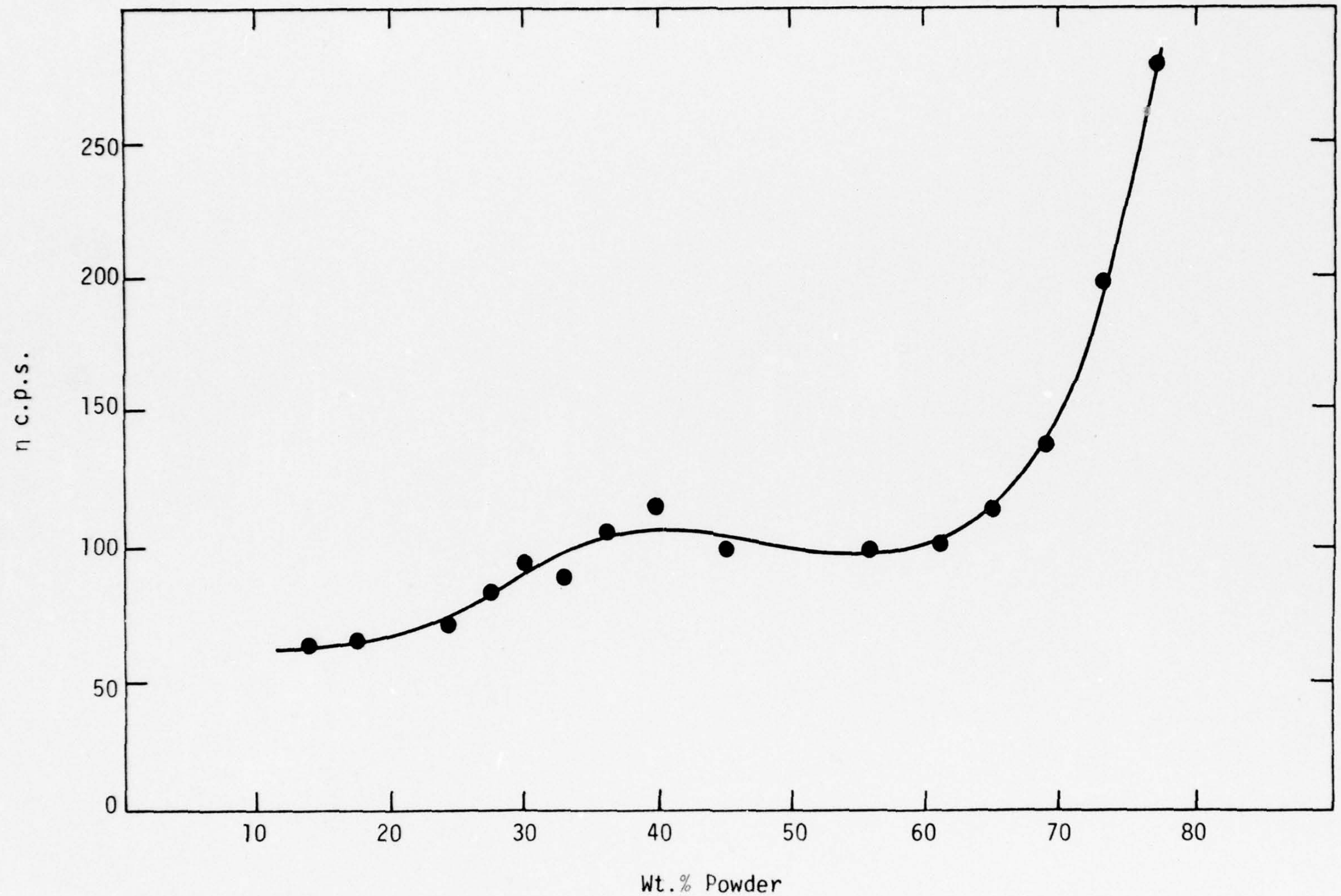

Figure 1. Viscosity vs. wt.% Powder at 48 hour mill time; 300 r.p.m.

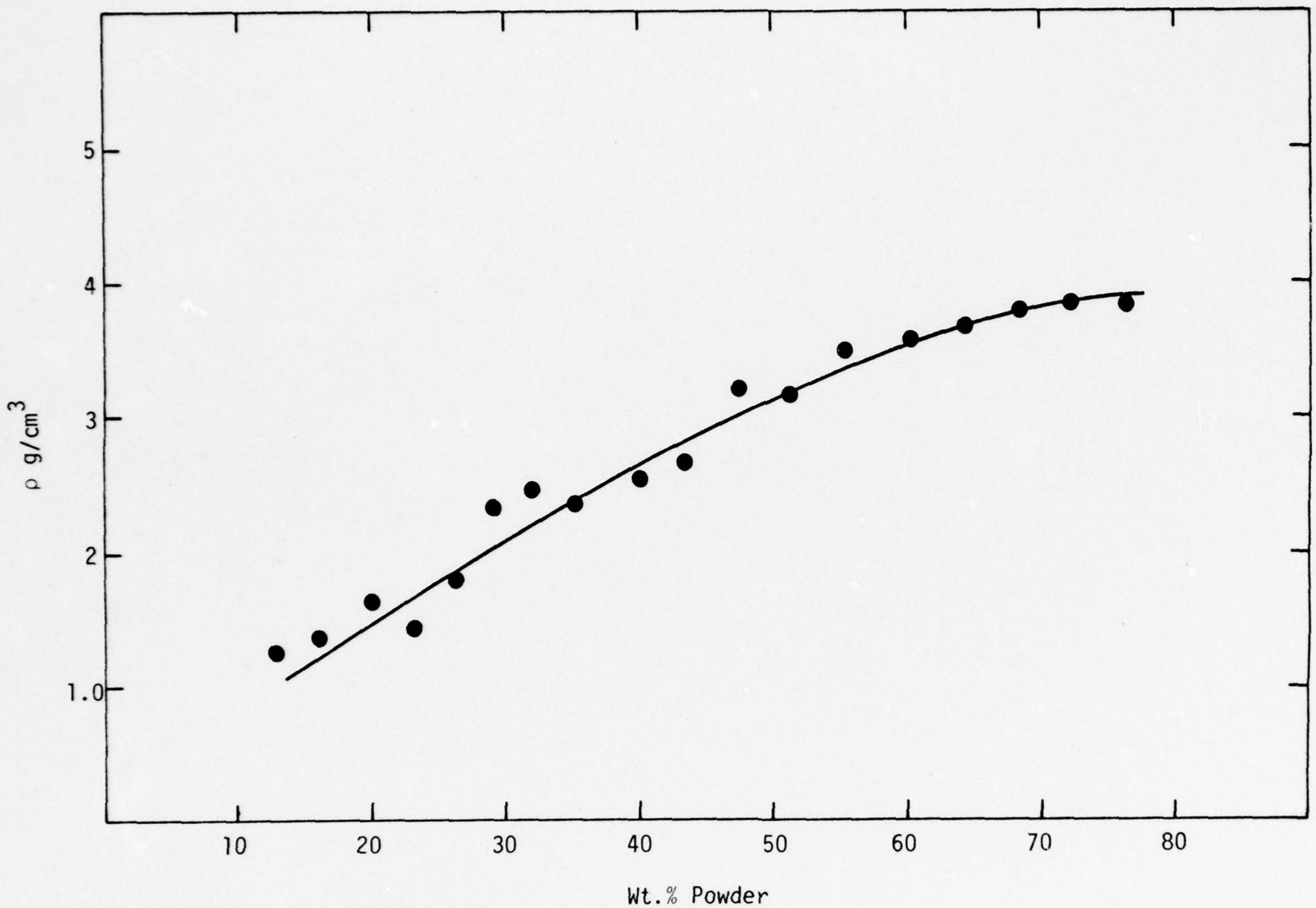

Figure 2. Green Density vs. wt.% Powder at 48 hours mill time.

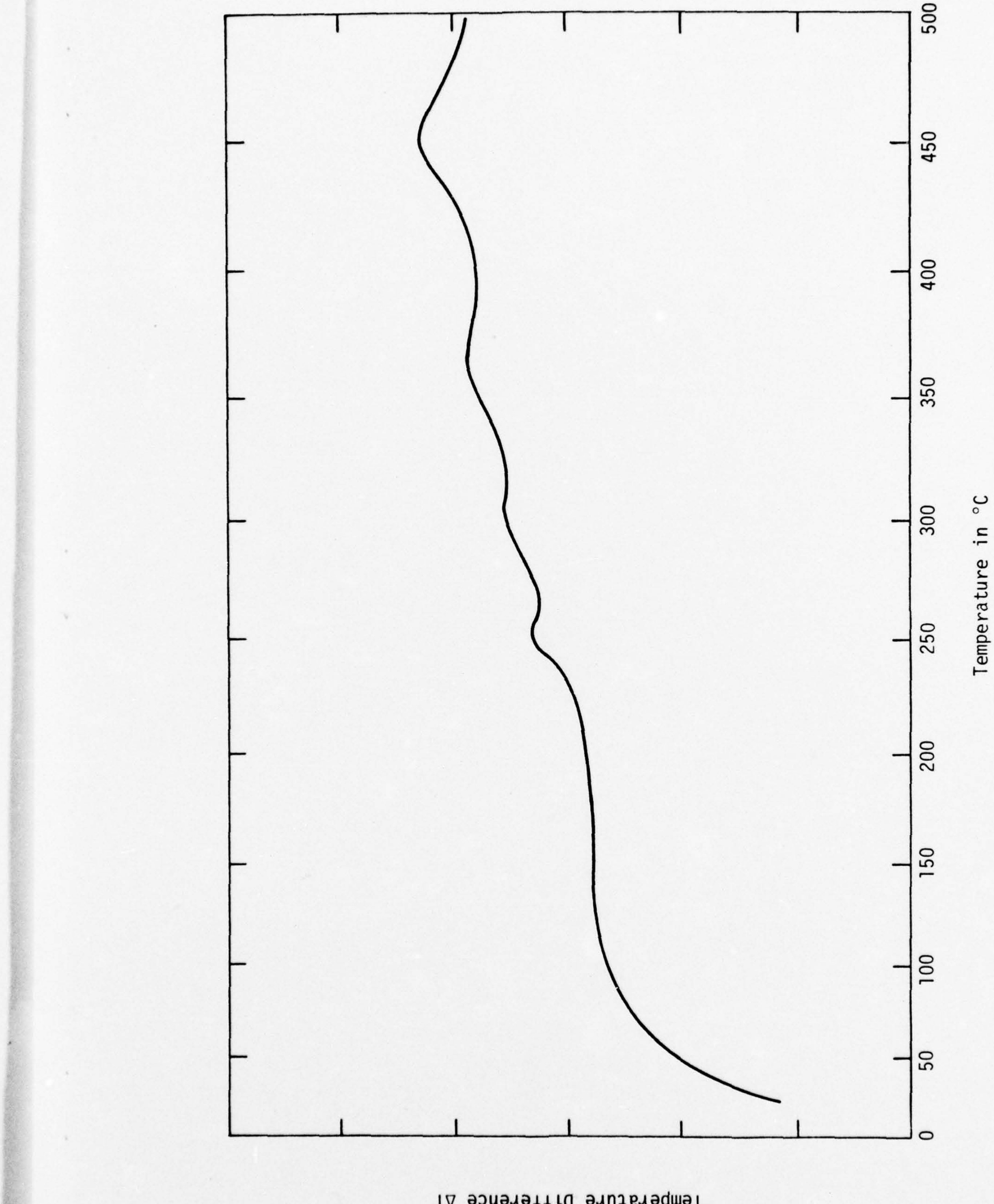

Figure 3. D.T.A. of PZT Tape.

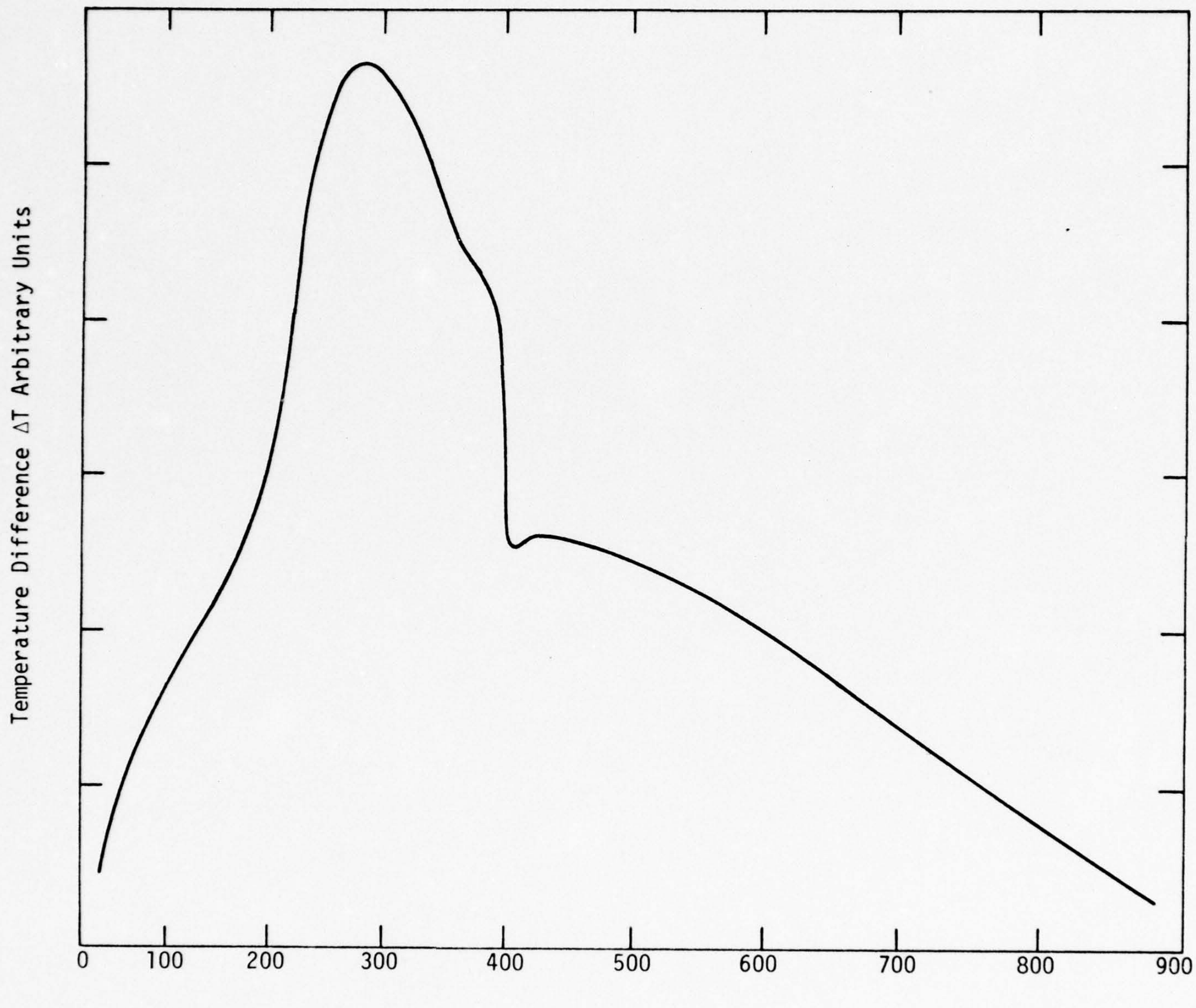

Figure 4. D.T.A. of Platinum Electrode Ink.

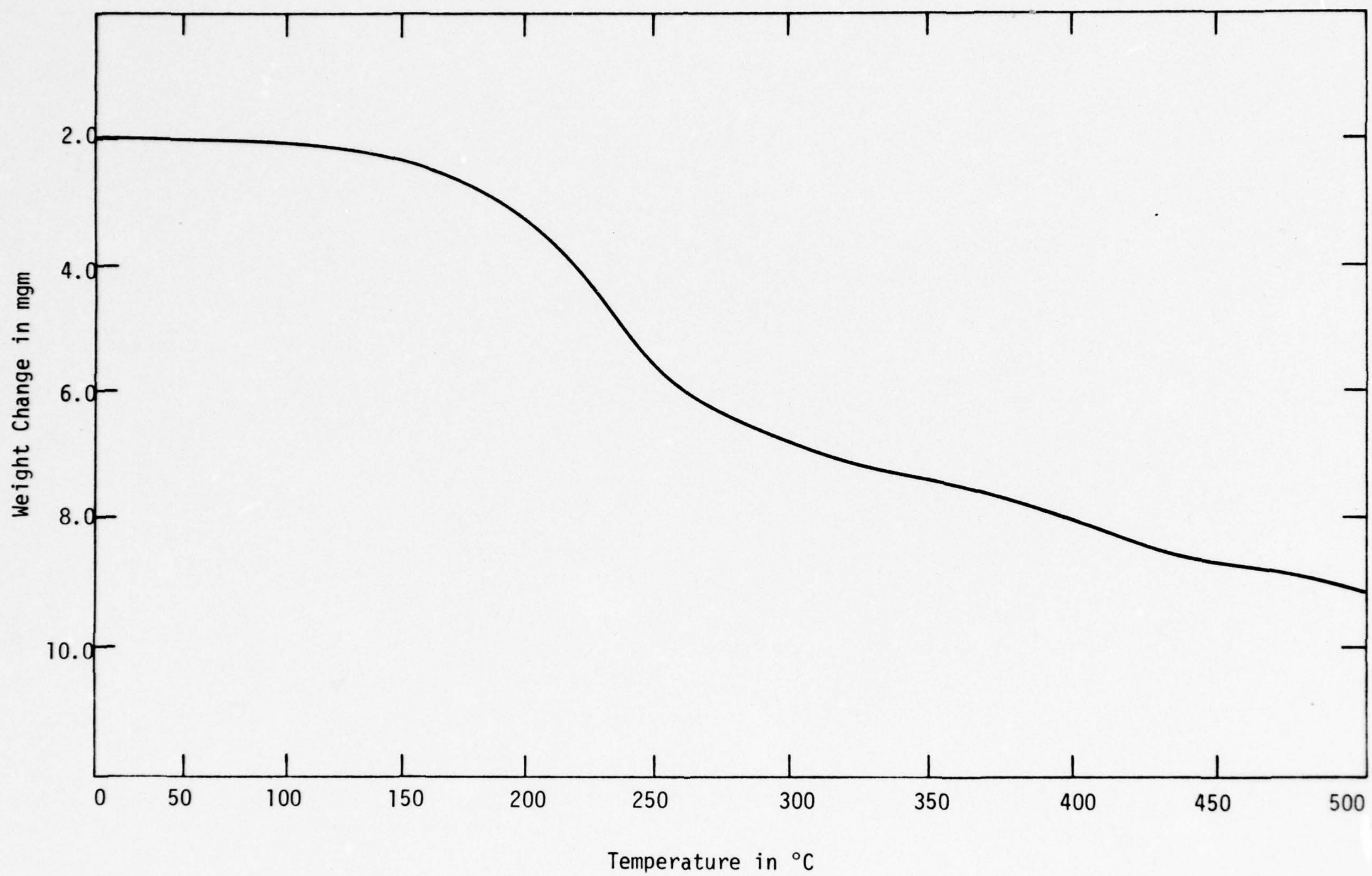

Figure 5. T.G.A. of PZT Tape.

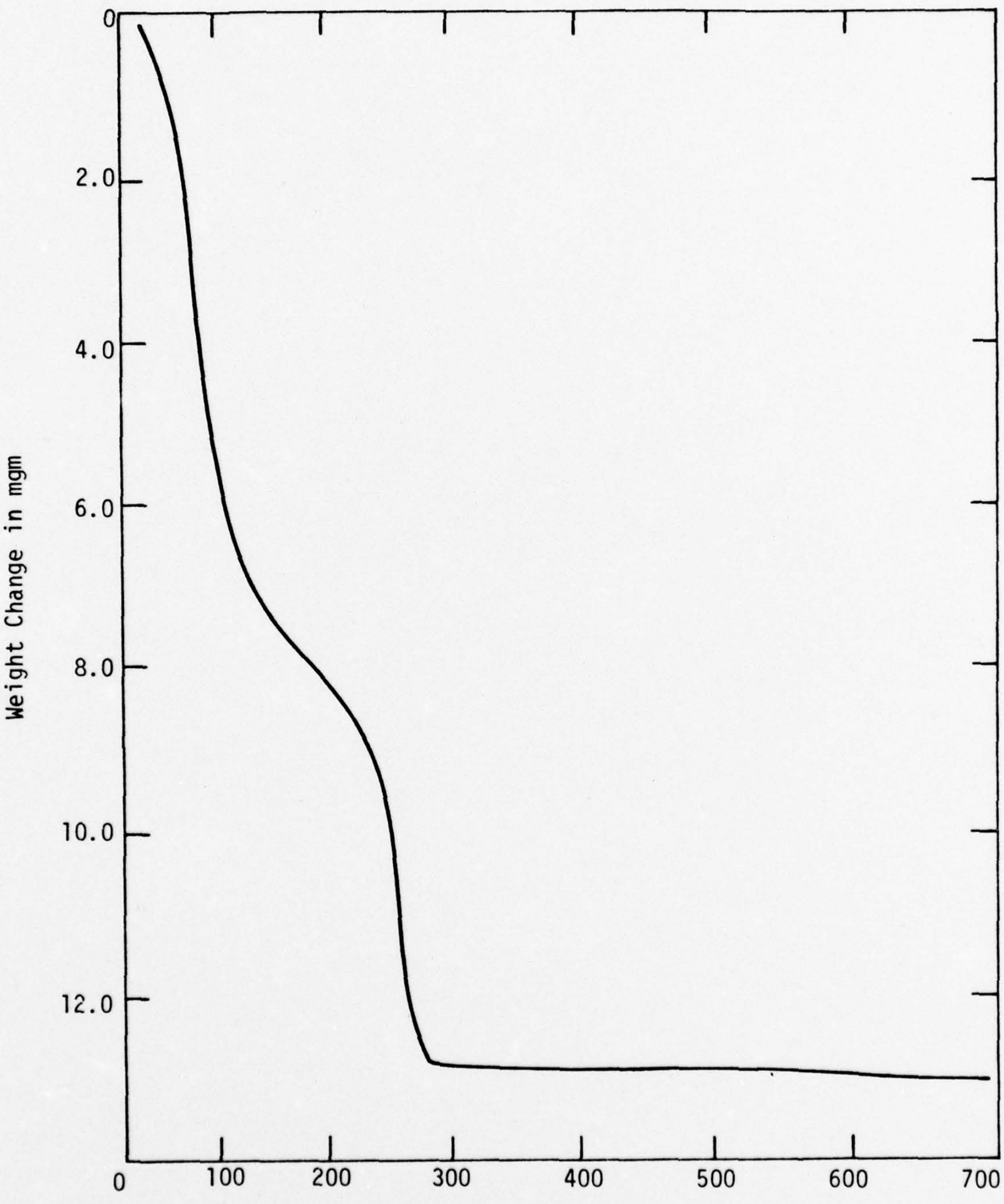

Figure 6. T.G.A. of Platinum Electrode Ink.

length of 4" width with green thickness in the range 2 - 20 mils. It will be supplemented by a standard commercial unit which has been donated to MRL by Carborundum Company and which will be delivered early in 1977.

One problem which has been evidenced by these early studies is the need for fine particles with a wide range of sizes, and the consequent need for long milling times with potential for excessive contamination from the milling media. We have constructed a new high energy mill, based on a commercial attritor-mill which uses a polyurethane jar and tungsten carbide grinding medium. This mill is capable of producing dispersions of powder and organic constituents in much shorter times and thus with much lower contamination levels than the present ball mills. Experiments are now proceeding to compare tapes made using conventional and high energy milling.

A commercial screen printer (Presco Model 251) is now on order and this machine will be used to print the electrode configurations for multilayer devices based on the tapes being developed.

3.1.3. Conventional Cold Pressing

Initial studies to establish firing and atmosphere control schemes have been carried through on conventional cold pressed samples die formed in a simple Carver Automatic press. To provide the facility required for pressing the large number of samples which will be required to compare tape cast and conventionally cold pressed and sintered samples, a 32 station Stokes Automatic Loading Rotary Press has been asquired through the DIPEC system. This machine is now being modified to accommodate a smaller number of stations with a wider range of specimen diameters.

Clearly it is undesirable for our group to become too heavily involved with very conventional processing techniques and it is our intention to confine this activity to providing essential base line samples for intercomparison with 'newer' processing methods.

To provide a further check against current industrial practice, we have arranged with Linden Laboratories, a commercial transducer manufacturer in the State College area to process limited batches of samples prepared in MRL for intercomparison with our own conventional and tape cast processing.

3.1.4. Hot Isostatic Pressing (Hardtle Technique)

A hot pressing vessel designed for operation with an internally heated hot zone 2" diameter x 4" long capable of continuous operation at 1250°C under 5000 psi pressure is nearing completion. All metal parts for the vessel

have been fabricated and machined; the internal furnace is nearing completion, and the pressure and temperature control equipment is now in place. Trial runs using this technique for the hot isostatic pressing of pre-sintered PZT compositions will commence early in 1977.

3.2. Thermodynamic Phenomenology

Two closely interrelated problems have been of major concern during the initiation of our phenomenological studies. The first concerns the development of techniques using the ADAGE computer graphics system to enable the visualization of polarization surfaces of constant Elastic Gibbs Free Energy for simple proper ferroelectrics with cubic perovskite prototype symmetry. The second concerns attempts to generate parameters in the Gibbs function which will describe the behavior of PZT type ceramics and in particular will model the morphotropic nature of the tetragonal:rhombohedral ferroelectric:ferroelectric phase transition in this system.

3.2.1. ADAGE Visualization of Polarization Surfaces

Symmetry dictates that the simple proper ferroelectric species which may evolve from the prototype m3m point symmetry of perovskite type materials are described by an Elastic Gibbs Free Energy which for zero applied stress takes the form

$$\begin{aligned}\Delta G = {} & A(P_1^2 + P_2^2 + P_3^2) + B(P_1^4 + P_2^4 + P_3^4) + C(P_1^2P_2^2 + P_2^2P_3^2 + P_3^2P_1^2) \\ & + D(P_1^6 + P_2^6 + P_3^6) + E(P_1^2P_2^4 + P_1^2P_3^4 + P_2^2P_1^4 + P_2^2P_3^4 + P_3^2P_1^4 + P_3^2P_2^4) \\ & + F(P_1^2P_2^2P_3^2) \end{aligned} \qquad (3.1)$$

Where $P_1P_2P_3$ are the components of electrical polarization with respect to the cubic axes 1, 2, 3.

The coefficients A, B, C,....F are in general functions of the temperature, and the expression 3.1 contains all allowed terms up to the 6th power in P.

Clearly 3.1 can be generalized when required to describe crystals under non zero stress by adding appropriate terms to take account of elastic and elasto-electric energy storage.

The conditions

$$\frac{\partial \Delta G}{\partial P_i} = E_i = 0 \qquad (3.2)$$

are required for stability.

Thus, from the family of equations generated by taking the partial derivatives of ΔG, with respect to P_1, P_2, P_3 the conditions upon the A, B,...F which give rise to stable solutions with non zero values of P_1, P_2, P_3 can be explored.

When values of A....F have been chosen which fit the observed evolution of ferroelectric phases (phases with non zero P_i) and which adequately describe the temperature dependence of P_s in these phases, a check can be made with the 'single domain' weak field dielectric properties which must be described by:

$$\frac{\partial^2 \Delta G}{\partial P_i \partial P_j} = X_{ij} \qquad (3.3)$$

where the X_{ij} are reciprocal susceptibilities of the various possible species. The equation 3.3 may be used at any level of Pi to describe the saturation of permittivity, however, if the values corresponding to the spontaneous polarization derived from 3.2 are substituted, then the family of X_{ij} values describes the 'weak field' single domain properties of that species.

For $BaTiO_3$, Devonshire (1, 2, 3) has shown that a good qualitative description of the whole ferroelectric phase system can be given with only four non zero parameters (A, B, C, D).

$$\left.\begin{array}{l} A = 5.10^{-5}\,(T-110) \\ B = -1.1 \times 10^{-12} \\ C = -1.4\,B \\ D = 0.61 \times 10^{-12} \end{array}\right\} \text{CGS Units} \qquad (3.4)$$

where only A carries temperature dependence.

A more quantitatively exact fit to the single domain polarization and dielectric permittivity can be obtained using the parameter values given by

Buessem, Goswami and Cross (4, 5). Namely:

$$\left.\begin{aligned} A &= 3.7 \times 10^{-5}\ (T-108) \\ B &= 5.8 \times 10^{-14}\ (T-120) - 2.5 \times 10^{-13} \\ C &= -7.4 \times 10^{-25}\ (T-120) + 3.7 \times 10^{-23} \\ D &= 4.0 \times 10^{-13} \\ E &= 6.0 \times 10^{-23} \end{aligned}\right\} \quad \text{CGS Units}$$

These were chosen to closely model the crystal properties near room temperature, and are adequate for all temperature down to -10°C. They would, however, require a non zero F value to correctly model the low temperature rhombohedral phase.

An obvious place to begin the study of three dimensional polarization surfaces, is to take the simple Devonshire expression and calculate directly the polarization contours which satisfy 3.1 (modified to include only the Devonshire parameters). In fact, of course, the calculation procedure can be greatly simplified through application of the symmetry requirements, only 1/48 of the solid surface need be determined, then the analogue feature of the ADAGE can be used to reconstruct the full surface by simple rotation operations.

In the vicinity of the upper phase transition at 120°C, the mutation of the polarization surfaces with decreasing ΔG can be seen in Figures 7a through f and the developing anisotropy of the surface at constant ΔG with decreasing temperature in Figure 8a through d. As expected, it is evident from Figure 7, that the lowest energy path from the cubic to tetragonal stabel phases at 120°C lies along any of the $\langle 100 \rangle$ directions.

The shapes of the surfaces at low ΔG values are also completely consistent with the known anisotropy of dielectric permittivity in the tetragonal polar phase, but give interesting new information as to the directional dependence of the rate at which the permittivity will saturate under high E fields.

To facilitate an understanding of the utility of 3-dimensional plots on AGADE, in which time is used to model the 4th dimension (ΔG) or (T), the ADAGE curves have been compared with a more conventional presentation of P_x, P_y and ΔG at constant and zero P_z. A movie has been filmed which makes a simple direct comparison, this film was shown at the recent Materials Research Society Meeting in Boston (November 1976).

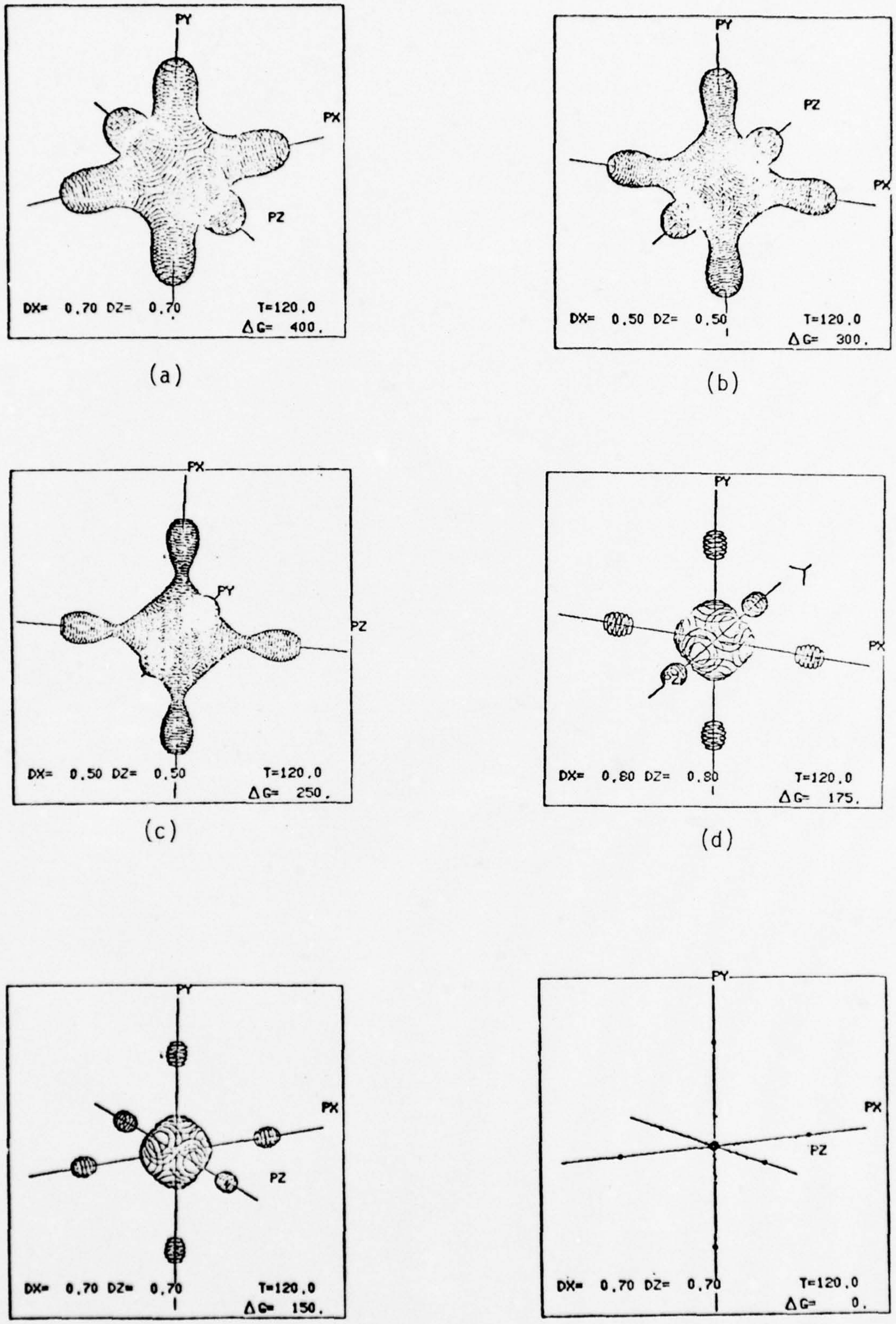

Fig. 7. Polarization surfaces in $BaTiO_3$ at 120°C as a function of decreasing Elastic Gibbs Free Energy ΔG.

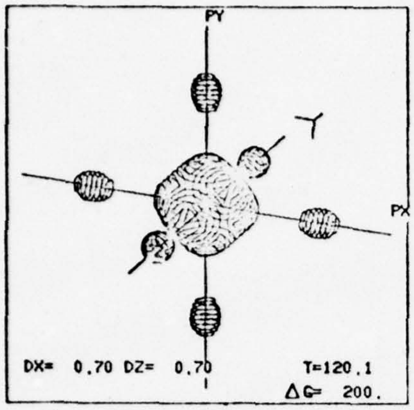

(a)

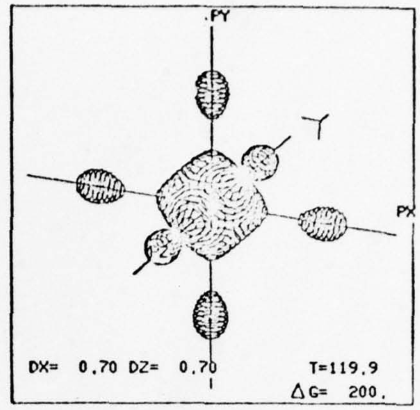

(b)

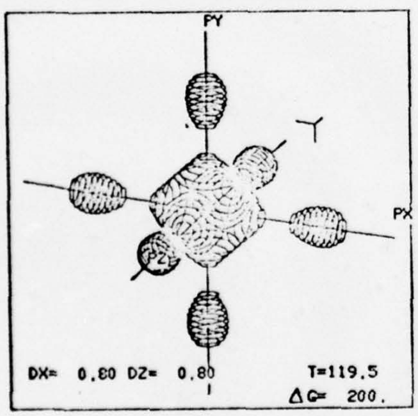

(c)

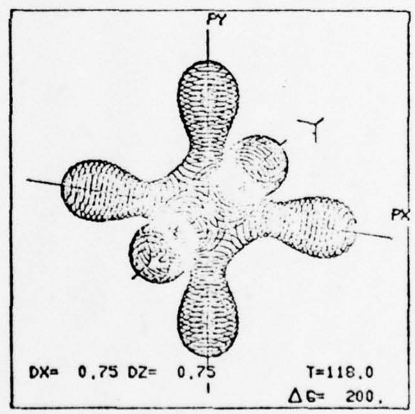

(d)

Fig. 8. Polarization surfaces in $BaTiO_3$ at on Elastic Gibbs Free Energy $\Delta G = 200$ as a function of temperature near 120°C.

The method is now being extended to the more interesting ferroelectric: ferroelectric phase changes at 0°C and -90°C. Two dimensional cuts of the polarization surface is 100 and 110 planes are being used to delineate the range in ΔG over which different ferroelectric phases coexist (ex. Figure 9) and to explore possible switching paths. The very marked anisotropy of the energy minimum evident in Figure 9, necessitates this preliminary step to avoid much useless computation.

It is anticipated that the full three-dimensional modeling for $BaTiO_3$ will be completed over the next three months, and this work will be presented at the American Ceramic Society meeting in April. To facilitate an extension of the same methods of solution to the morphotropic transitions in PZT, the program has been written to take the full family of constant and temperature coefficients which may be necessary.

3.2.2. Modeling of Morphotropy

Perhaps the most unusual and important feature in the $PbZrO_3$:$PbTiO_3$ system is the occurrence of a morphotropic boundary between rhombohedral and tetragonal ferroelectric phases at a composition near $Pb(Zr_{0.52}Ti_{0.48})O_3$.

A full set of 'Devonshire' parameters which would allow the correct modeling of the single domain dielectric properties in PZTs near this composition would be most valuable, however, single crystals of these compositions have never been grown and the task of modeling from only the 'averaged' ceramic properties is indeed daunting.

One objective of our study has been to use the ADAGE graphics system to test out how restrictive the condition of morphotropy is upon the range of possible parameters in the elastic Gibbs function.

Using the full analogue capability of the system, it is possible to control eight parameters in the program by simple dial settings. For initial study, these parameters were chosen to be:

A_0

α the temperature coefficient of A i.e., $A = A_0 + \alpha T$.

B_0

β the temperature coefficient for B i.e., $B = B_0 + \beta T$.

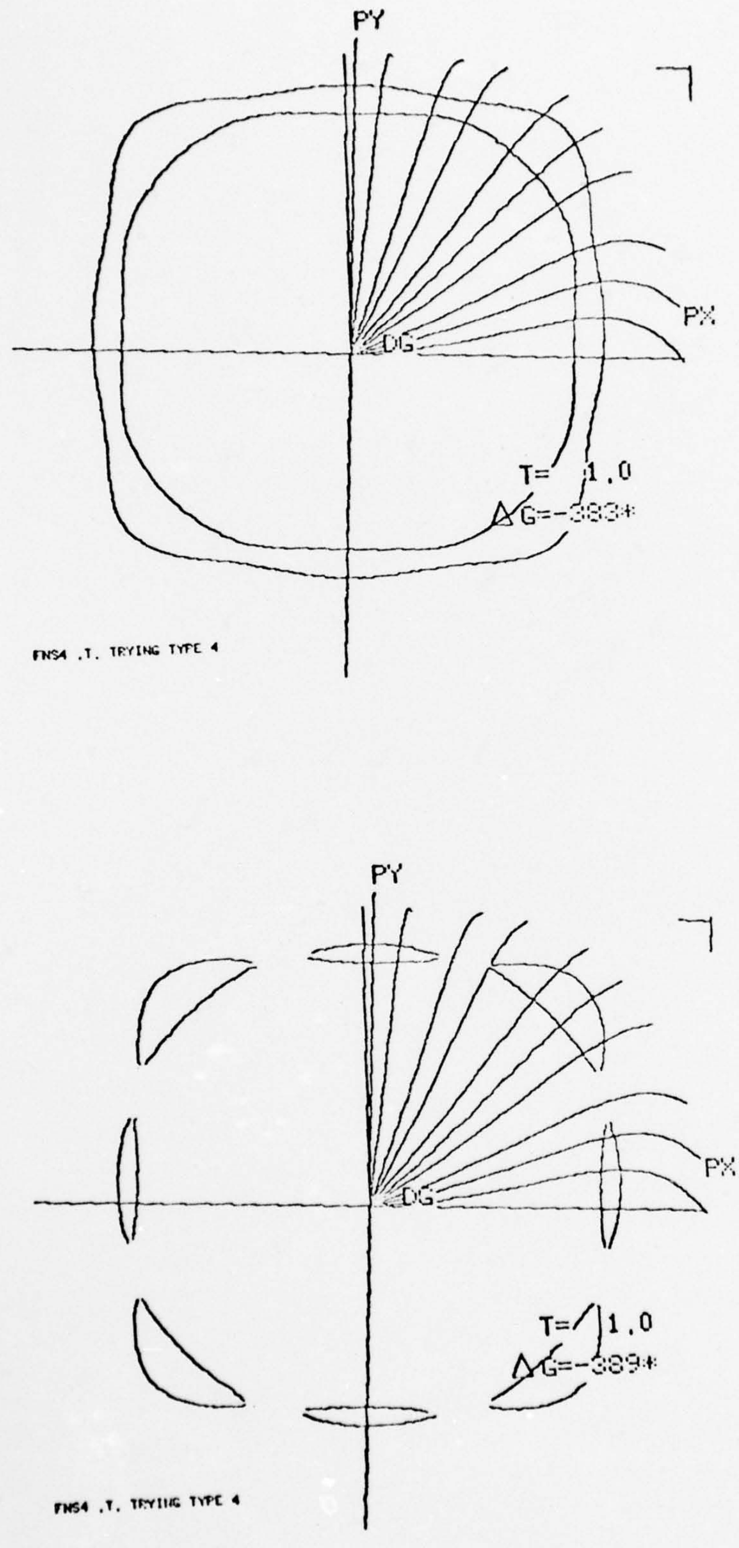

Fig. 9. Polarization contours in the Pz = 0 plane at temperature T = 1°C
Close to the tetragonal: ortherhombic phase change.

D

E

F_o

γ the temperature coefficient for F i.e., $F = F_o + \gamma T$.

The coefficient C is set at a value $C = \phi B_o$, the multiplier ϕ can be reset by a single program step. In ADAGE, the whole program can be retrieved page by page on the display console and replaced or updated by keystroke entry.

For phase boundary calculations, the ADAGE is used in a split screen format. The program proceeds as follows:

(1) Taking values of the constants set by the analogue dials, equations 3.2 are solved for a sequence of T values from $T > T_c$ to a lower program limit. The corresponding values of ΔG vs T are plotted on the right hand half screen. The line of lowest ΔG values corresponds to the stable ferroelectric phase (tetragonal, orthorhombic or rhombohedral) over that temperature range.

(2) From the ΔG vs T the phase transition temperatures are read off. The program then increments one of the higher order constants to a new value, say $F_o + \Delta F$, the ΔG vs T plot is repeated and the new phase transition temperatures read off. By repeatedly incrementing F_o, a plot is then built up of the F vs T phase diagram.

Both the increment and the range for F_o, or any other higher order variable can be set in the program instructions. Each ΔG vs T plot takes ∿40 seconds seconds, so that for 40 increments a F vs T plot can be built up in ∿3 minutes A typical phase diagram executed in this way is shown in Figure 10.

The program set up in this way has the following advantages:

(a) A wide range of settings of the constants can be quickly checked for the corresponding stable phases.

(b) Since the ΔG vs T plot is constantly under observation, parameter combinations which give tetragonal stable, and rhombohedral metastable combinations without any interleaving orthorhombic phase can be rapidly ascertained.

(c) For these parameter combinations, dial settings can be trimmed to make the temperature evolution of the two phases closely parallel.

R-O ICRO= 0

PHI= -0.446
B(T)= 85.7
E = 100.0
FS = -100.0
F(T) = -0.5
TMIN= 50.1

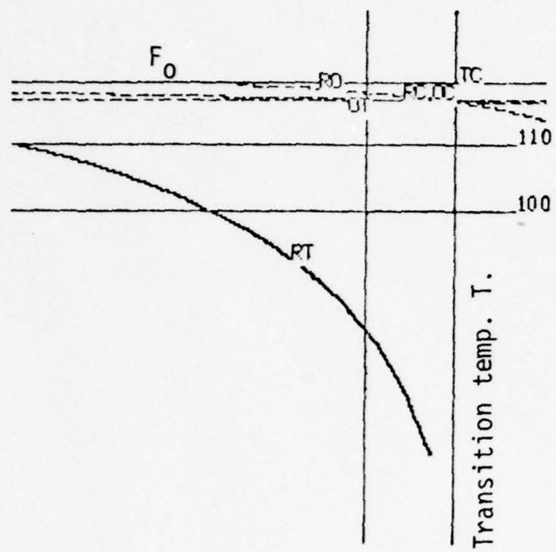

FLG4 IS .F.
FLG13 IS .F.
LEVEL2 IS .F.
FLGWRT=.F. FNS(10)

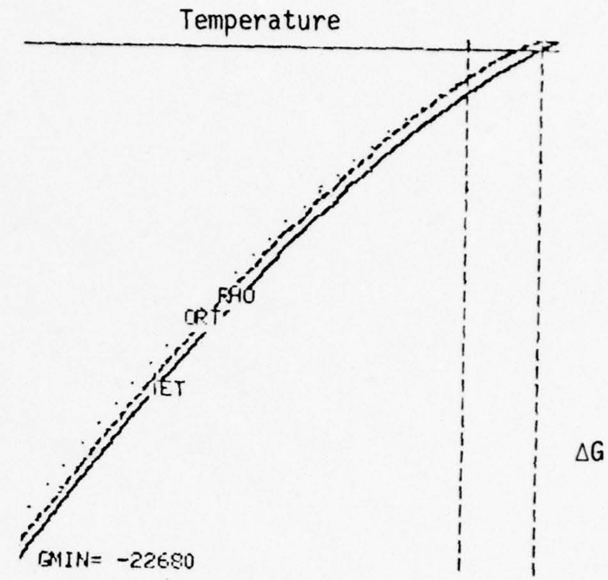

(a)

Fig. 10. Adage presentation of the direct calculation of a phase diagram in F_o is T space.

(a) ΔG vs T: final plot at the limit of F.

(b) Calculated F_o vs T phase diagram.

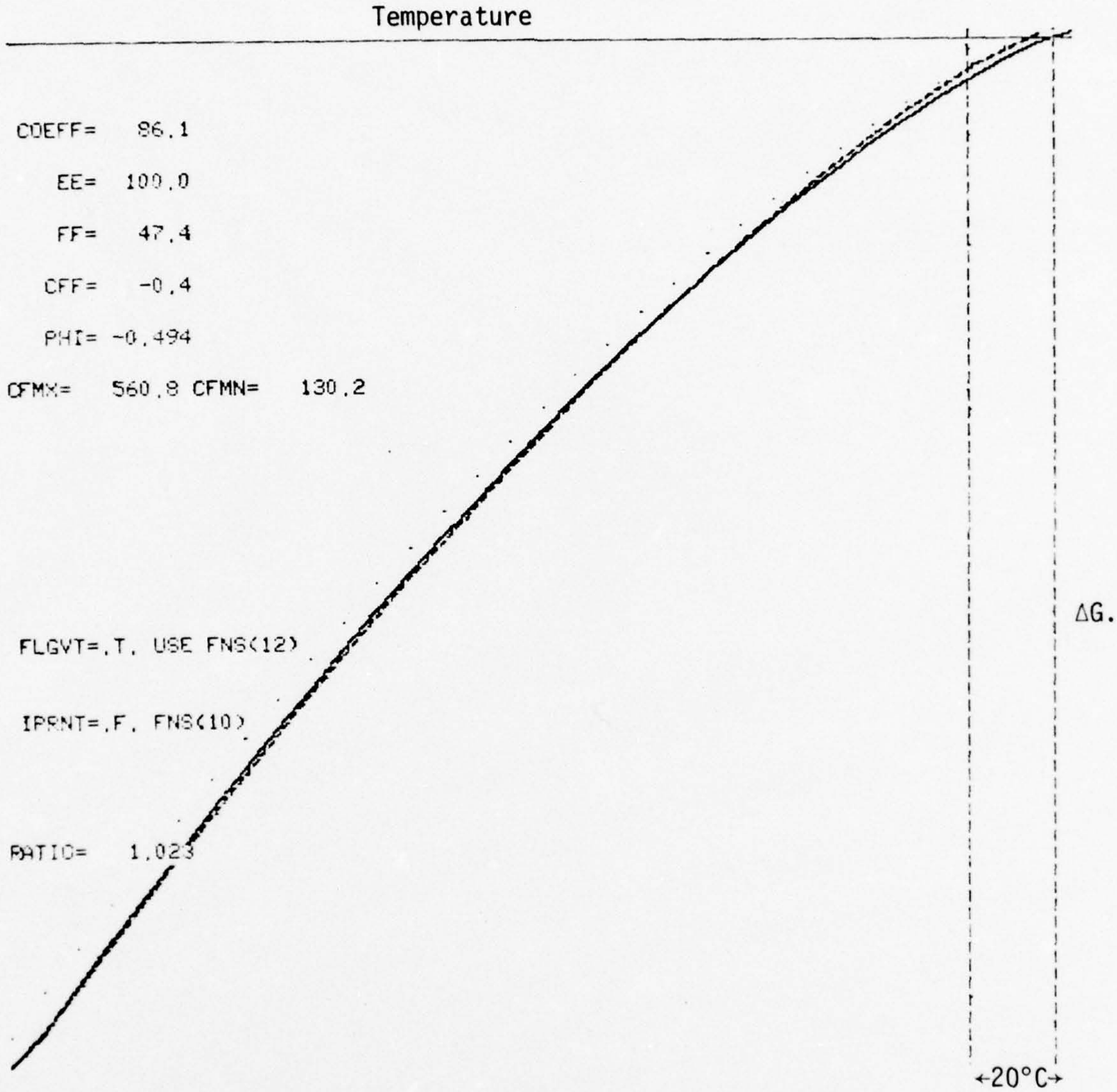

Fig. 10 c. Enlarged ΔG vs T plot for parameter combination which exhibits good morphotropy between Tetragonal and Rhombohedral stable phases.

(d) Incrementing one of the higher order parameters it becomes clear that only when the two phase boundary lines are very closely parallel on the ΔG vs T plots does the F_0 vs T diagram show reasonable morphotropy.

Few combinations of parameters give tetragonal and rhombohedral phases without interleaving orthorhombic stability, and for these, the requirements for morphotropy are highly restrictive.

The next step in these calculations is now to chose the scale factors so that the observed morphotropic combinations fit as closely as possible with the observed PZT phase diagram, i.e.,

(i) to chose the Curie temperature and Curie constant (A_0 and α) to fit the high temperature dielectric measurement on cubic PZTs.

(ii) to chose a composition dependence of the higher order parameter so as to most closely mimic the observed morphotropy in PZT, without inducing extraneous phase changes at points remote from the transition.

For combinations which best describe the observed diagram, polarizations and average permittivities will be calculated for comparison with observed values. Once the parameters have been properly fixed, then we may go on to use the earlier program to plot the three-dimensional polarization surfaces for PZT so as to be able to better study the trajectories for morphotropic switching.

3.3. Electrostriction Transducers

Following discussions with G. Kino at the MRC review in La Jolla in June 1976, it was decided to explore the electroelastic response of a number of multilayer dielectric capacitors. Since the group at Stanford have demonstrated the unusual capability of a conventional K 6,000 monoblock* capacitor to generate strong ultrasonic signals in water the mechanism of coupling obviously requires elucidation.

---

*Monoblock is a registered tradename of the Erie Technological Products Company.

In multilayer ceramic configurations which can be realized, for example, by the doctor blade technique very thin layers of high permittivity perovskite type dielectrics can be fabricated. With modern formulations, where the saturation of the permittivity has been controlled, large values of polarization can be induced by quite low voltages. Thus, even in the absence of any poling or domain reorientation the purely electrostrictive deformations may be large.

For a $BaTiO_3$ based formulation, which has been engineered so that the 'Curie range' is close to room temperature it might be expected that the longitudinal dimension change $\Delta\ell/\ell$ be given by:

$$\Delta\ell/\ell = Q_{11}P_I^2 \tag{3.6}$$

and for the transverse effect

$$\Delta\ell/\ell = Q_{12}P_I^2 \tag{3.7}$$

where Q_{11} and Q_{12} are the appropriate polycrystal (averaged) electrostriction constants, and P_I the induced electric polarization under applied E field.

To confirm the electrostrictive nature of the response, it was decided to use a simple commercial dilatometer to measure directly the dimension change $\Delta\ell$ as a function of applied voltage for a number of capacitor dielectrics both in monoblock multilayer form, and in single thin sheet form.

Arrangements were made with Erie Capacitor Company to obtain batches of their K 6,000 and K 5,500 monoblocks in 1, 2 and 3 μF capacitances without polymer dip coating. The company also supplied a number of samples of a proprietary cylindrical multilayer geometry in K 2,300 and K 6,000 dielectrics. Centre Engineering of State College also supplied a number of multilayer elements in their K 2,600, K 2,000 and K 8,000 formulations, again without protective coating.

Considerable care must be exercised in selecting commercial units for study. In many instances the active (electroded) region does not cover the whole area of the capacitor surface, often additional passive layers are laid over the

surfaces for environmental protection. For smaller capacitors also, it is often the case that internal connection is omitted to alternate electrodes. For these measurements a representative number of samples in each batch were sectioned and studied under high magnification in the scanning electron microscope. By applying voltage to the capacitor under study the changing contrast reveals at once any unconnected plates. Electrode separations were measured using both SEM, and on polished sections on an optical reflection microscope.

For the transverse $\Delta\ell/\ell$, individual tubes or plates were measured directly in the dilatometer. In the longitudinal mode, however, even the 50 layer capacitor is too thin to give a large enough $\Delta\ell$ to measure in the primitive dilatometer setup presently used. To provide some preliminary data for this mode, composite samples were made up by carefully polishing the surfaces to flatness on a number of elements, then laminating them into a stack using very thin coatings of epoxy cement.

The dimensions of samples, the experimentally measured maximum values of $\Delta\ell$, and the appropriate strain $\Delta\ell/\ell$ are summarized in Table 2.

To make some comparison with the predictions of equation 3.6 and 3.7, it is necessary to measure the polarization as a function of applied field, for each sample. This was carried through in two ways:

(1) To give an indication of the 'reversible' component of the total polarization, the weak field slope permittivity $\partial D/\partial E|E \rightarrow 0$ was measured as a function of E. The total reversible polarization $P_1(R)$ at a field level E, was then calculated from

$$P_1(R) = \int_0^{E_1} \varepsilon_R(E)dE.$$

(2) Using the Sawyer and Tower method, dielectric hysteresis loops were generated with a slow wave sweep of 1 Hz, and the maximum polarization read off from the tip of the loop for each required level of applied field.

By measuring the strain $\Delta\ell/\ell$ at a sequence of increasing field levels, a set of Q_{ij} values was calculated from the relations

$$\Delta\ell/\ell = Q_{11}P_T^2 \quad (3.8) \qquad \text{and} \qquad \frac{\Delta\ell}{\ell} = \left[\int_0^{E_1} \varepsilon_0\varepsilon(E)dE\right]^2 \quad (3.9)$$

These data are tabulated in Tables 3 and 4.

Table 2a. Dilatation Data for Samples of Erie Commercial Multilayer Capacitor Dielectrics.

Erie Multilayers

Sample Description	Dimensions	Transverse		Longitudinal	
		$\Delta\ell$ Measured	$S_{11}=\Delta\ell_1/\ell_1$	$\Delta\ell$ Measured	$S_{33}=\Delta\ell_3/\ell_3$
Cylinder 1 K 2,300	ℓ 1.6 cm d 43 μm	1.47 μm 200 V	9.2×10^{-5}		
Cylinder 2 K 6,000	ℓ 4.95cm d 42 μm	4.93 μm 160 V	9.95×10^{-5}		
Plate 1 K 6,000	ℓ 0.89cm d 48.6 μm	0.88 μm 200 V	9.76×10^{-5}	0.356 μm	4.0×10^{-4}
Plate 2 K 6,000	ℓ 0.89cm d 48.6 μm	1.02 μm 200 V	1.28×10^{-4}		
Plate 3 K 5,500	ℓ 0.89cm d 29.6 μm	0.85 μm 200 V	0.96×10^{-4}	0.42 μm	5.96×10^{-4}
Plate 4 K 5,500	ℓ 0.90cm d 34.6 μm	1.54 μm 200 V	1.7×10^{-4}	0.47 μm	5.3×10^{-4}
Plate 5 K 5,500	ℓ 0.66cm d 24.6 μm	0.55 μm 180 V	8.3×10^{-5}	0.47 μm	5.3×10^{-4}
Plate 6 K 5,500	ℓ 0.88cn d 34.6 μm	1.29 μm	1.47×10^{-4}		

Table 2b. Dilatation Data for Samples of Commercial Multilayer Capacitor Dielectrics from Centre Engineering.

Sample Description	Dimensions	Transverse $\Delta\ell$ Measured	Transverse $S_{11}=\Delta\ell_1/\ell_1$	Longitudinal $\Delta\ell$ Measured	Longitudinal $S_{33}=\Delta\ell_3/\ell_3$
Plate 1 K 2,600	ℓ 1.11 cm d 24.6 μm	0.93 μm 200 V	8.42×10^{-5}	0.235 μm	7.8×10^{-4}
Plate 2 K 2,600	ℓ 1.13 cm d 29.6 μm	0.80 μm 200 V	7.07×10^{-5}	0.373 μm	4.5×10^{-4}
Plate 3 K 2,000	ℓ 1.15 cm d 62.6 μm	0.73 μm 200 V 2.3 μm 600 V	6.36×10^{-5} 2.02×10^{-4} 600 V	0.55 μm	2.3×10^{-4}
Plate 4 K 2,600	ℓ 0.61 cm d 14.5 μm	0.09 μm 210 V 0.52 μm 610 V	1.5×10^{-5} 8.5×10^{-5}		
Plate 5 K 8,000	ℓ 0.62 cm d 19.6 μm	0.94 μm 200 V	1.52×10^{-4}	0.24 μm 120 V	6.20×10^{-4} 120 V

Table 3. Calculated Electrostriction Constants Q_{11}, Q_{12} for Erie Multilayer Dielectrics.

Sample	Bias	From K Measurements		From Hysteresis Curve	
		Q_{12}	Q_{11}	Q_{12}	Q_{11}
Cylinder I	40 V	8.83×10^{-3}		1.49×10^{-2}	
	80 V	6.36×10^{-3}		1.86×10^{-2}	
	120 V	4.21×10^{-3}		1.78×10^{-2}	
	160 V	1.83×10^{-3}		1.6×10^{-2}	
	200 V	1.79×10^{-3}			
Average		4.60×10^{-3}		1.68×10^{-2}	
Cylinder II	40 V	4.1×10^{-2}			
	80 V	4.5×10^{-2}			
	120 V	4×10^{-2}			
	160 V	3.4×10^{-2}			
Average		4×10^{-2}			
Square Plate 1	40 V	2.05×10^{-2}	12×10^{-2}	1.31×10^{-2}	4.75×10^{-2}
	80 V	2.38×10^{-2}	13×10^{-2}	1.88×10^{-2}	6.52×10^{-2}
	120 V	2.40×10^{-2}	13.3×10^{-2}	1.84×10^{-2}	6.58×10^{-2}
	160 V	2.36×10^{-2}	13.8×10^{-2}		
	200 V	2.41×10^{-2}	14×10^{-2}		
Average		2.32×10^{-2}	13.2×10^{-2}	1.68×10^{-2}	5.95×10^{-2}
Square Plate 2	40 V	7.21×10^{-3}	5.54×10^{-2}	7.11×10^{-3}	3.75×10^{-2}
	80 V	7.39×10^{-3}	5.24×10^{-2}	4.98×10^{-3}	3.10×10^{-2}
	120 V	7.94×10^{-3}	5.36×10^{-2}	3.21×10^{-3}	2.44×10^{-2}
	160 V	8.44×10^{-3}	5.43×10^{-2}		
	200 V	8.95×10^{-3}	5.56×10^{-2}		
Average		7.99×10^{-3}	5.43×10^{-2}	5.1×10^{-3}	3.10×10^{-2}

Table 3 (continued)

Sample	Bias	From K Measurements Q_{12}	From K Measurements Q_{11}	From Hysteresis Curve Q_{12}	From Hysteresis Curve Q_{11}
Square Plate 3	40V	3.40×10^{-2}	9.53×10^{-2}		
	80 V	2.66×10^{-2}	8.30×10^{-2}		
	120 V	2.46×10^{-2}	7.65×10^{-2}		
	160 V	2.30×10^{-2}	7.27×10^{-2}		
	180 V	2.27×10^{-2}	7.17×10^{-2}		
	Average	2.62×10^{-2}	7.98×10^{-2}		
Square Plate 4	40 V	4.83×10^{-3}	3.62×10^{-2}		
	80 V	5.38×10^{-3}	3.47×10^{-2}		
	120 V	6.03×10^{-3}	3.61×10^{-2}		
	160 V	6.02×10^{-3}	3.07×10^{-2}		
	Average	5.57×10^{-3}	3.44×10^{-2}		
Square Plate 5	40 V	1.91×10^{-2}			
	80 V	1.84×10^{-2}			
	120 V	1.90×10^{-2}			
	160 V	1.83×10^{-2}			
	200 V	1.88×10^{-2}			
	Average	1.87×10^{-2}			

Table 4. Calculated Electrostriction Constants Q_{11}, Q_{12} for Centre Engineering Multilayer Dielectrics.

Sample	From K Measurements			
	Bias	Q_{12}	Bias	Q_{11}
S - 1	40 V	8.84×10^{-3}	40 V	5.37×10^{-2}
	80 V	6.24×10^{-3}	80 V	5.89×10^{-2}
	120 V	5.16×10^{-3}	120 V	5.41×10^{-2}
	160 V	5.96×10^{-3}	160 V	5.63×10^{-2}
	200 V	6.28×10^{-3}	200 V	5.75×10^{-2}
	Average	6.5×10^{-3}	Average	5.61×10^{-2}
S - 2	40 V	3.89×10^{-3}	50 V	4.73×10^{-2}
	80 V	4.65×10^{-3}	100 V	4.37×10^{-2}
	120 V	6.55×10^{-3}	150 V	4.34×10^{-2}
	160 V	5.94×10^{-3}	200 V	4.26×10^{-2}
	200 V	6.45×10^{-3}		
	Average	5.50×10^{-3}	Average	4.43×10^{-2}
S - 3	40 V	4.9×10^{-2}	100 V	1.06×10^{-1}
	80 V	3.67×10^{-2}	200 V	1.02×10^{-1}
	120 V	3.20×10^{-2}		
	160 V	2.87×10^{-2}		
	200 V	2.82×10^{-2}		
	Average	3.49×10^{-2}	Average	1.04×10^{-1}
S - 4	110 V	2.44×10^{-2}		
	210 V	1.88×10^{-2}		
	Average	2.16×10^{-2}		
S - 5	40 V	4.75×10^{-3}	40 V	2.18×10^{-2}
	80 V	4.71×10^{-3}	60 V	2.09×10^{-2}
	120 V	4.74×10^{-3}	80 V	2.08×10^{-2}
	160 V	4.77×10^{-3}	100 V	2.03×10^{-2}
	200 V	4.69×10^{-3}	120 V	2.11×10^{-2}
	Average	4.73×10^{-3}	Average	2.10×10^{-2}

It is evident from Figures 11, 12, 13 and 14 which plot $\Delta\ell/\ell$ vs P^2 derived from 3.9, that this relation is qualitatively satisfied for all the high K materials.

The average of the seven sets of measurements made on the high K samples give, using relation 3.9

$$Q_{11} = (6.7 \pm 3.7) \times 10^{-2} \ m^4/coul^2$$
$$Q_{12} = (1.8 \pm 0.7) \times 10^{-2} \ m^4/coul^2 \qquad (3.8)$$

These may be compared to the average values for ceramic $BaTiO_3$ given as

$$Q_{11} = 6.32 \times 10^{-2} \ m^4/coul^2$$
$$Q_{12} = 1.80 \times 10^{-2} \ m^4/coul^2 \qquad (3.9)$$

Considering the very wide variations in composition among the different materials, it is quite surprising that the constants are so close to those for pure $BaTiO_3$. Thus it does appear probable that normal electrostriction is, in fact, the major contributor to dimension change under field, and that the Erie K 6,000 composition is not unique in its striction properties.

For simple electro-mechanical motion linear activators, it would appear that the Erie K 5,500 material is capable even in present form of generating displacive strains $\sim 6 \times 10^{-4}$ at voltages $\sim$200 volts applied. With 1 mil layers which can certainly be doctor bladed in this material the voltage could be further reduced to $\sim$100 volts.

In systems where capacitive loading is important, the lower K 2,000 material from Centre Engineering could offer significant advantage because of its very high dielectric breakdown strength.

Because of the small size of the structures doctor bladed for capacitor applications, it is difficult with our present generation dilatometer to make direct comparison to the PLZ materials of present transducers.

If, however, as seems reasonable, it is accepted that most perovskites can be processed to form multilayer structures without serious degradation of properties (in fact, usually with significantly enhanced effective dielectric

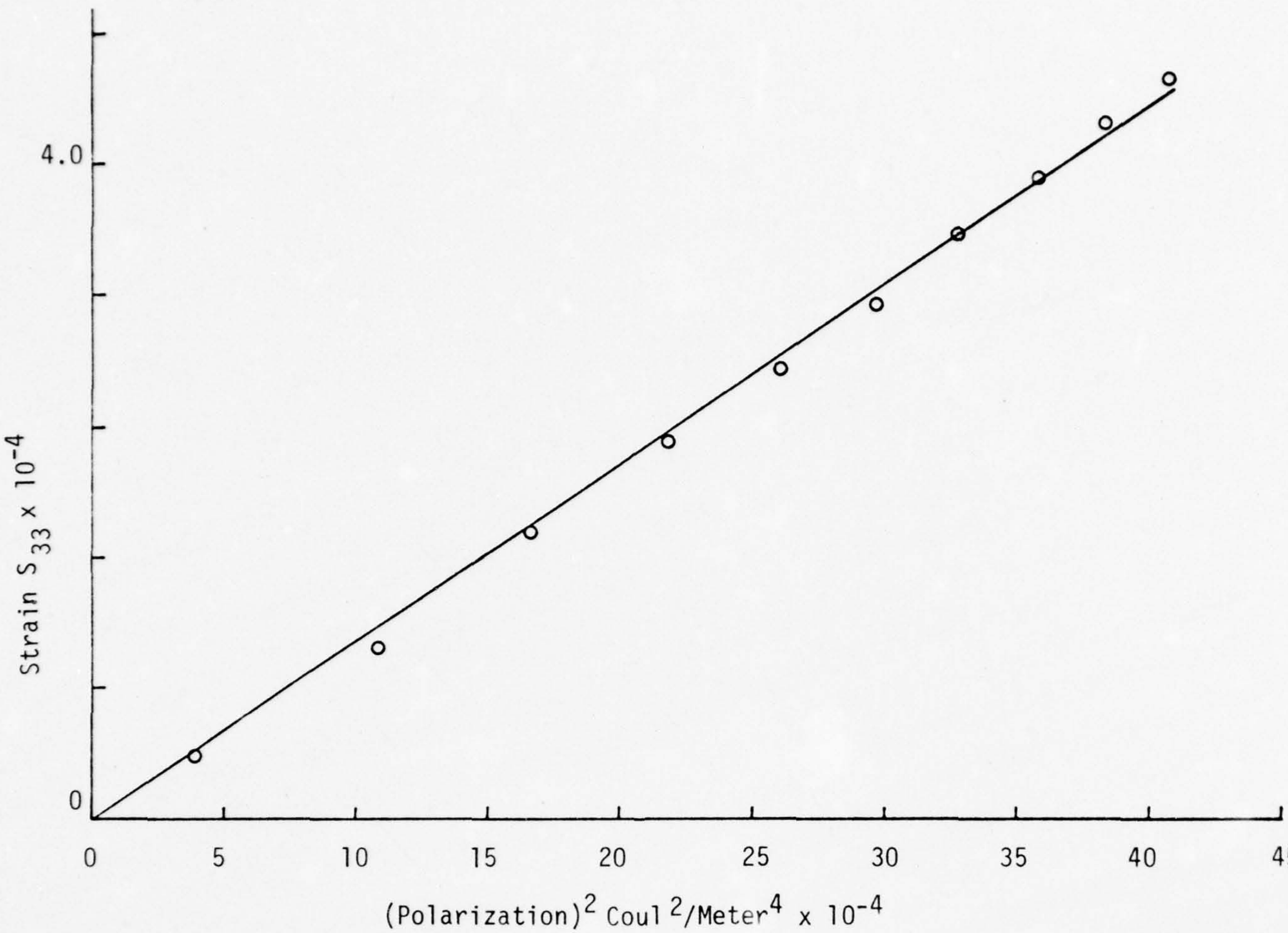

Fig. 11a. Electrostriction in Erie K6,000 (Longitudinal)

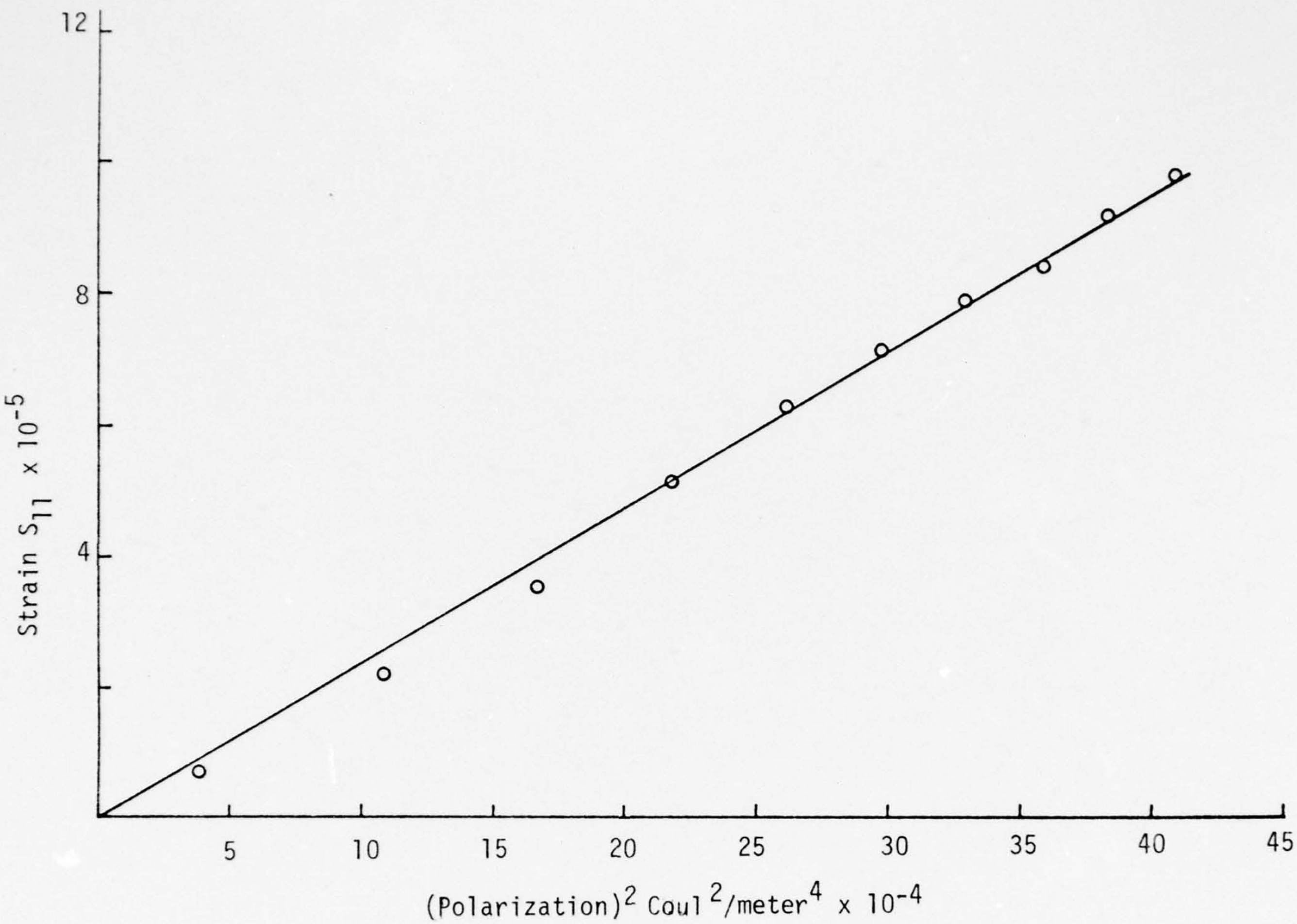

Fig. 11b. Electrostriction in Erie K6,000 (Transverse)

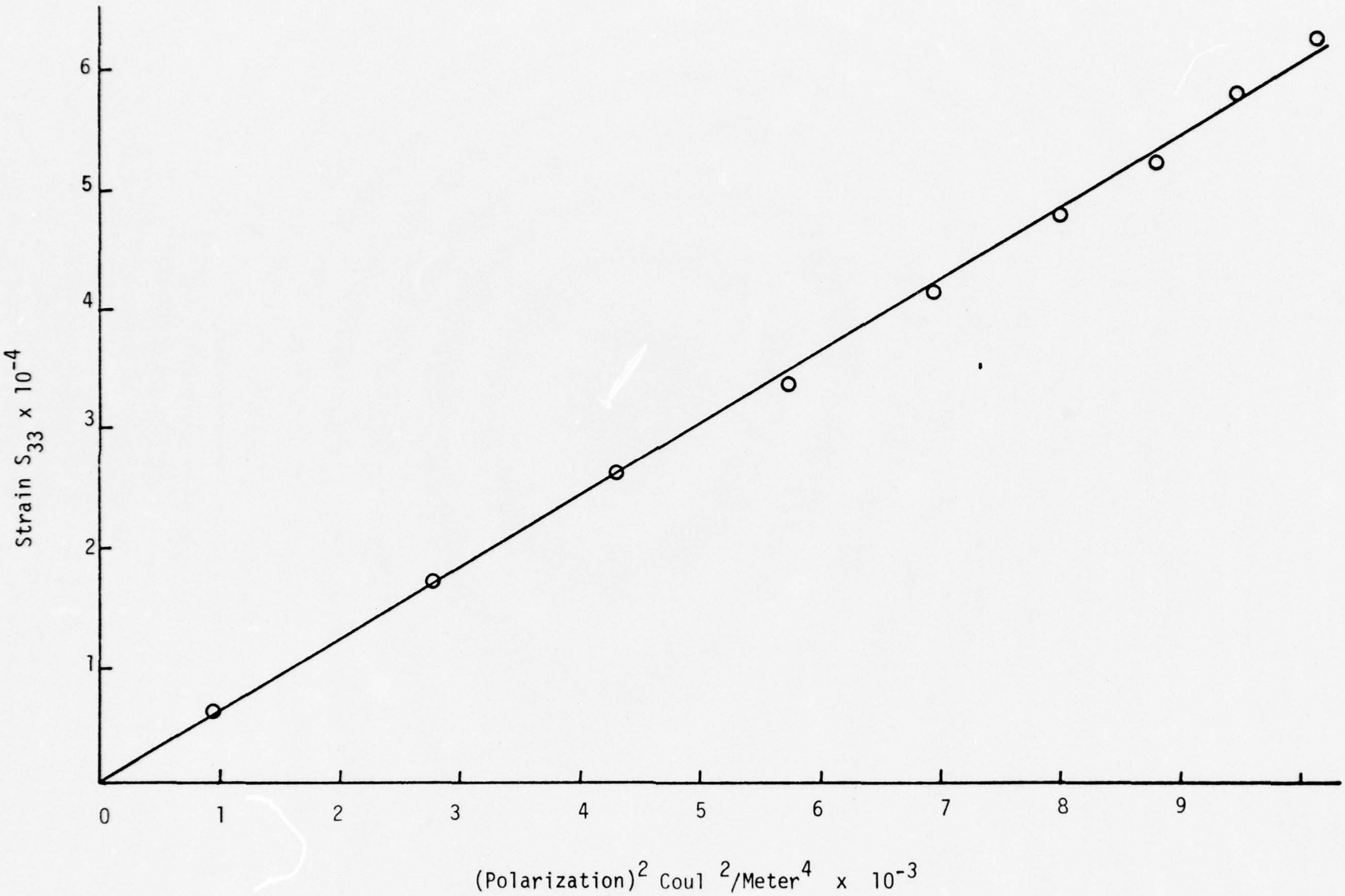

Fig. 12a. Electrostriction in Erie K-500 (Longitudinal).

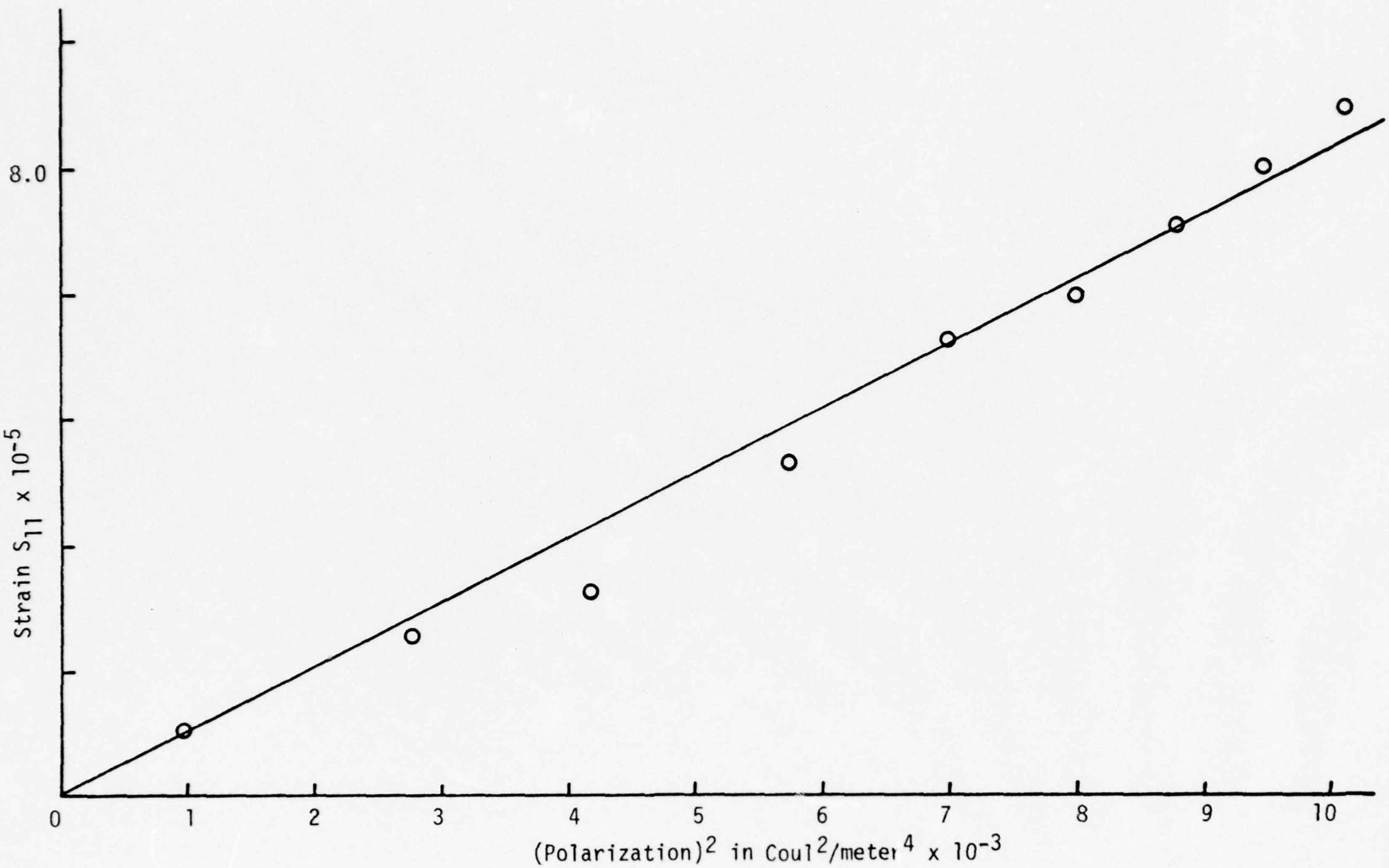

Fig. 12b. Electrostriction in Erie K5,500 (Transverse)

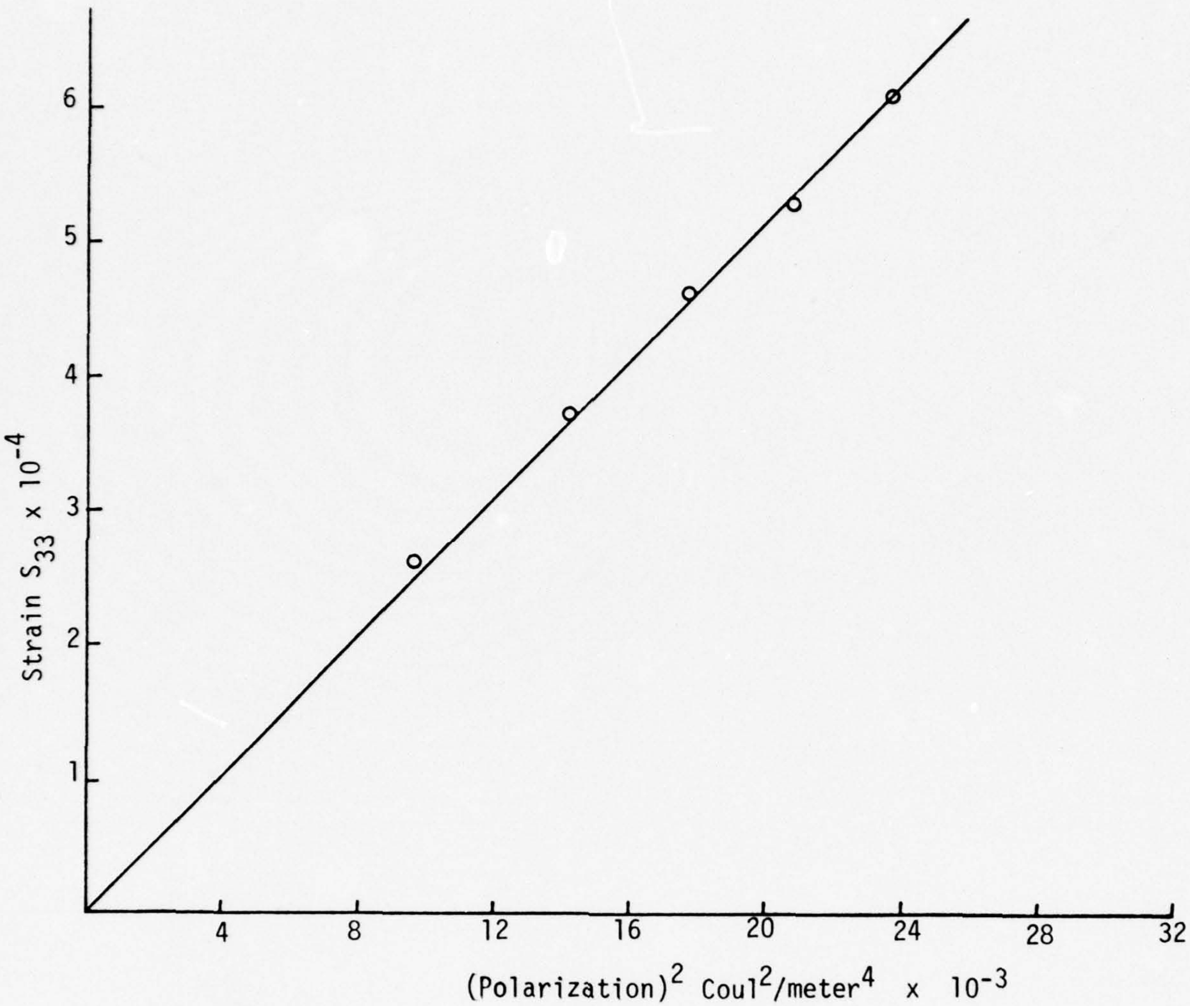

Fig 13a. Electrostriction in Centre Engineering K8000 (Longitudinal)

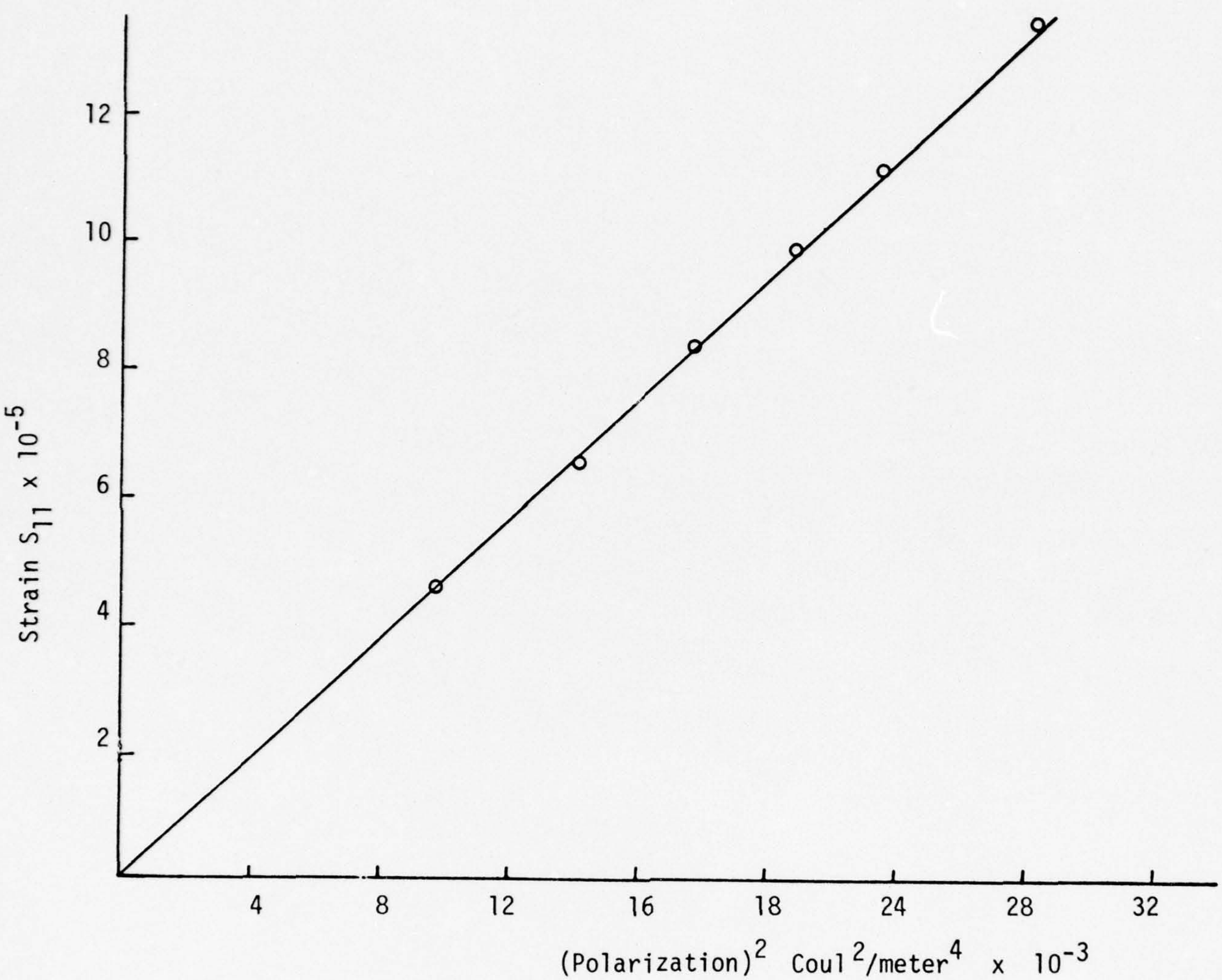

Fig. 13b. Electrostriction in Centre Engineering K8000 (Transverse).

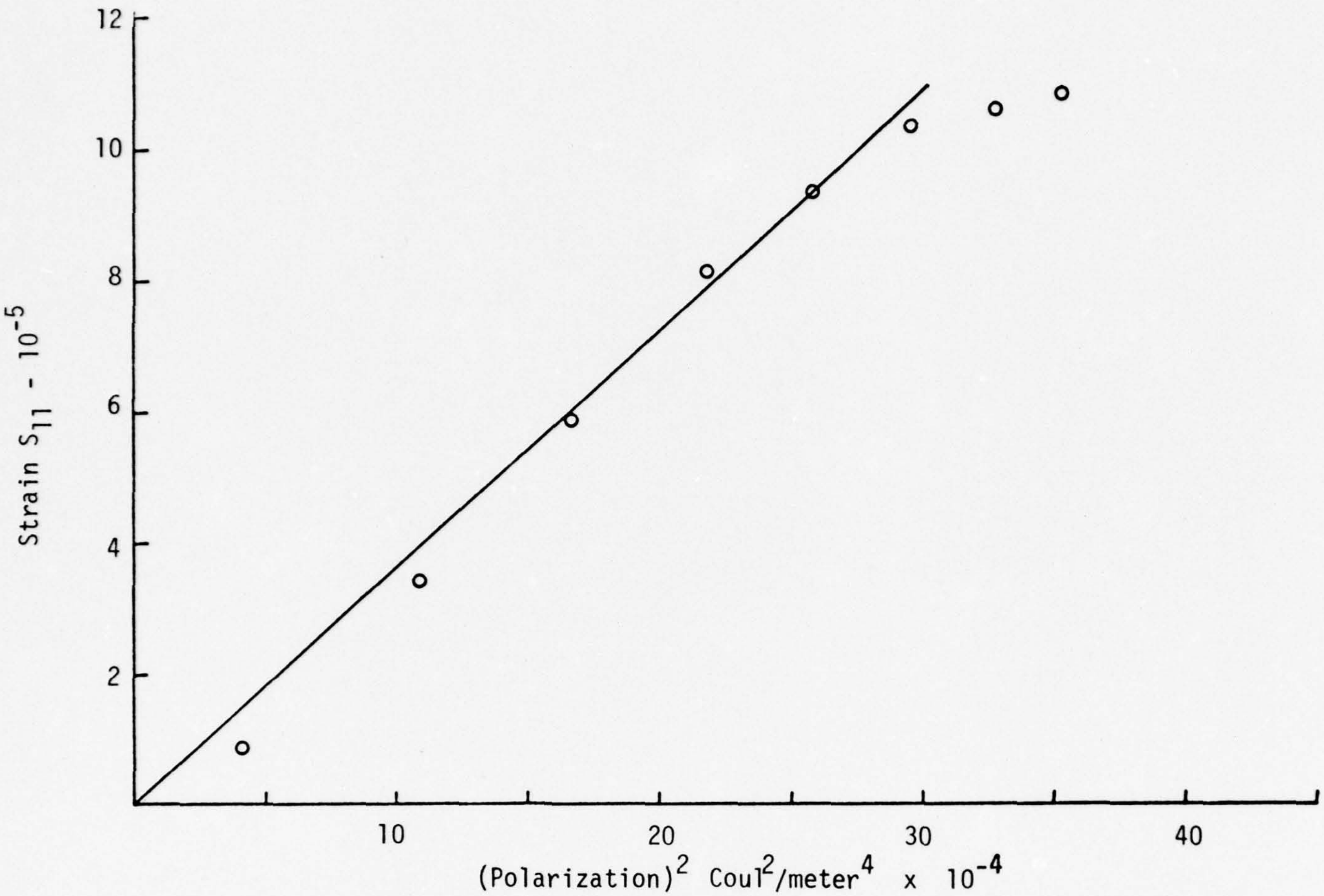

Fig. 14. Electrostriction in Cylindrical multilayer Erie K6000.

strength) it is possible to go ahead and make intercomparison between the bulk materials by operating the electrostriction ceramics at much higher voltage, but allowing for the fact that drive voltages can be suitably tailored in later manufacture.

On this basis we have made initial comparison of a number of new high voltage ceramic dielectrics in the electrostriction mode, and a conventional hard PZT (Channel 5800) which is recognized by the fabricators of adaptive optics to have properties most compatible with their requirements. Of special interest in this case is the total available distortion $\Delta\ell/\ell$, the stability of the field induced distortion, and the reproducibility under cyclic drive conditions.

Initial tests on a $BaTiO_3$:$NaNbO_3$ high voltage formulation developed in our laboratory show transverse strain $\sim 2.5 \times 10^{-4}$ at fields ~ 50 kv/cm well below the breakdown field (200 kv/cm) for this material in multilayer from. Because of the graded dielectric saturation in this composition, there is a wide range of linear response with an effective $d_{31} \sim -120 \times 10^{-12}$ V/meter. The reproducibility of the complete deformation were as evidenced in Figure 15, which was taken upon a virgin sample not previously subjected to cycling.

It is in the area of dimensional stability and reproducibility where the electrostriction device compares most favorably with PZT. Using a Channel 5800 ceramic which has an effective $d_{31} = -128 \times 10^{-2}$ m/V, with a drive of 14 kv/cm which is required to produce a similar total deformation, initial deaging on the first cycles makes it impossible to measure the dimension change on our dilatometer.

Even after 3 cycles, the material creeps some 0.5 μmeters/cycle and requires more than 20 cycles to establish reproducible cyclic behavior (Figure 16).

Reapplication of fields after a short resting period give reproducibility much more rapidly but with longer aging between drive cycles there is evidence that the initial dimensional creep re-emerges.

In a rather more recent study (6) we have been developing in cooperation with the Sprague Electric Company a family of PLZT dielectric bodies for high voltage operations. Because of the ability to chose the field strength for antiferroelectric:ferroelectric and antiferroelectric:paraelectric switching by composition modification in this family, it is possible to engineer formulations almost completely free from dielectric saturation (7,8).

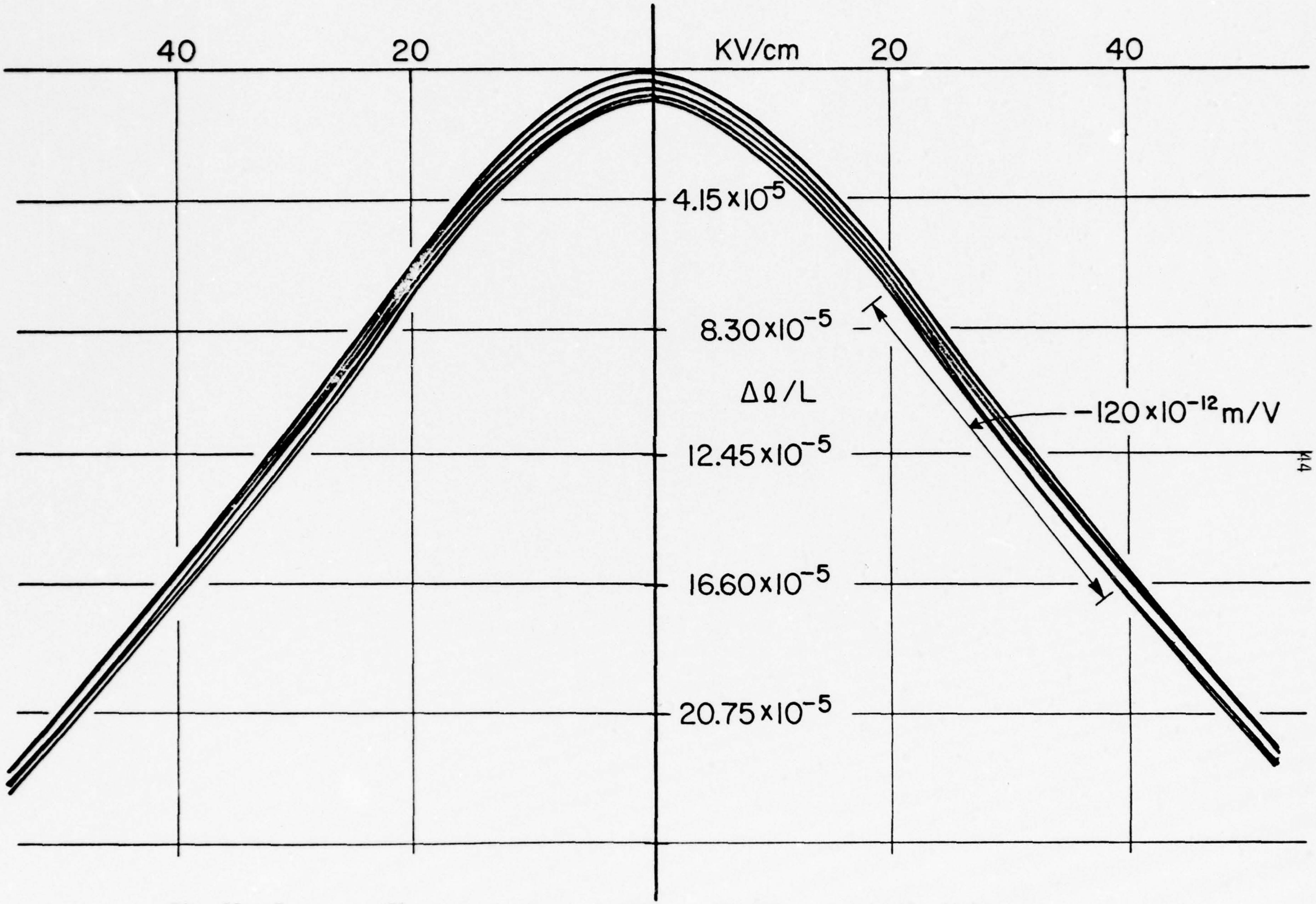

Fig. 15. Transverse Electrostriction in $BaTiO_3$: $0.05NaNbO_3$ under cyclic field.

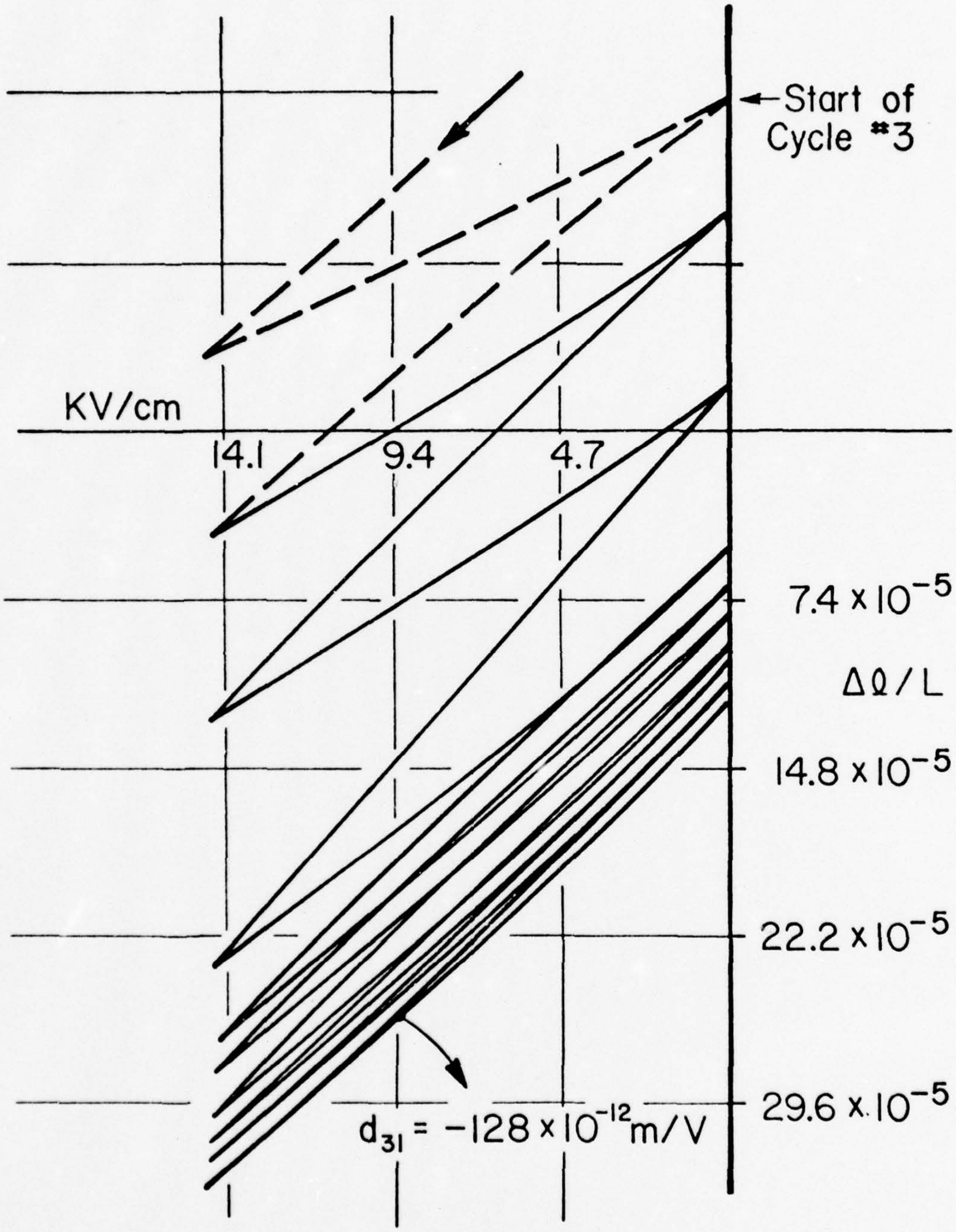

Fig. 16. Piezoelectric response in Channel 5800 under high cyclic field

Preliminary dilatometer studies upon several of these formulations (Figure 17) show that these dielectrics merit further study.

3.4. New Materials

3.4.1. New Ferroelectric Crystals with High Paraelectric Symmetry

To be of use in conventional ceramic form with randomly axed crystallites, new materials for piezoelectric applications must have:

(1) High prototype symmetry leading to ferroelectric phases with many alternative orientations in the domain states.

(2) High ferroelectric Curie temperature: Through the empirical Kurtz - Abrahams relations for simple proper ferroelectrics (9), the high T_c is necessarily accompanied by high P_s in the ferroelectric species, large ionic displacement:large spontaneous strain: and high intrinsic single domain piezoelectricity.

The perovskite family with its highest m3m prototype symmetry is an obvious choice for initial study, and an immense volume of work has been carried out (10) investigating multi-component perovskite oxide compounds for ferroelectric activity. Recently, however, Politova and Venevtsev (11) have given preliminary information about some 50 new perovskite compounds in the composition families

$$A_2^{2+}B^{2+}TeO_6$$

$$(A^{2+}A_3^{3+})B^{1+}TeO_6$$

$$(A_3^{3+}A^{1+})B^{2+}TeO_6$$

A^{2+} may be Ba, Pb, Sr, Ca or Gd
A^{3+} may be Bi or La
A^{1+} may be Na or Li
B^{2+} may be Mg, Co, Zn, Mn, Cd or Ca
B^{1+} may be Na or Li

Many of these compounds show phase changes at high temperatures, some with large dielectric anomalies and it is concluded that they are ferroelectric or antiferroelectric transitions. Certainly, qualitatively it might be expected

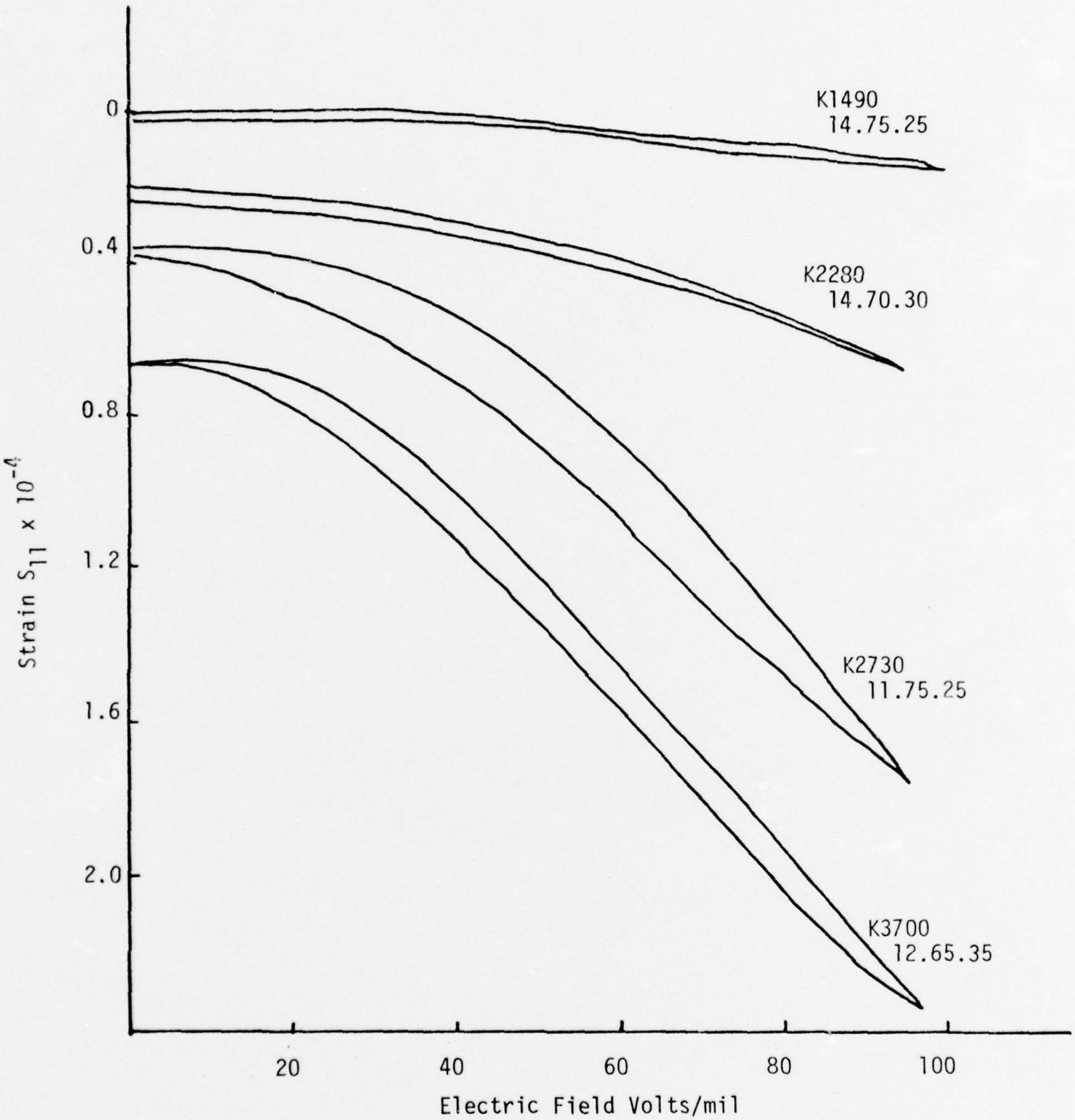

Fig. 17. Preliminary data of "Electrostrictive". Strain in PLZT dielectric compositions

that the samll highly charged Te^{6+} ion, if it can be stabilized in an oxygen octahedral environment, would give rise to large deformations and thus to strongly polar or antipolar phases with high Curie temperature. Unfortunately, in the earlier Russian study, no definitive experiments are carried through which would distinguish ferroelectric from antipolar behavior.

It was decided to make up a range of the more interesting compounds reported to have high transition temperatures in powder form and to use the powder SHG test to screen out quickly acentric phases for further study.

Tellurium based chemicals must be processed with some care because of the toxic properties of this element. All weighing, batch mixing and grinding operations were carried out on a laminar flow bench using respirator and plastic gloves. Firing was conducted in a small dedicated tubular globar furnace contained in a chemical exhaust hood.

In this manner, powders of the compounds listed in Table 5 were prepared. X-ray powder patterns were taken for each compound, and in all cases perovskite or distorted perovskite structures were identified. Since many of these new perovskite compounds are not in the x-ray powder index, small quantities of each were supplied to the Penn State group responsible for updating the powder file data and detailed indexing was carried out on these materials for the reference file.

The optical SHG system, which is perhaps the most sensitive technique for determining acentricity, has been significantly modified and improved from the original design given by Kurtz (12) though the basic principle is similar.

Light from a pulsed Nd glass laser (Control Data 1040A) filtered to remove any background triggering light is split at a weakly reflecting surface. Part is picked up by a semiconductor photo diode which identifies the incident waveform, part is incident on the sample.

Forward scattered light from the sample is passed through a narrow band filter stack which accepts only the 530 μ harmonic frequency. Back scattered light is collected by a parabolic mirror and also passes through the filter stack to the detector. A cooled EMI 9558 photomultiplier is used as detector. A small pre-amplifier matches the output impedance of the multiplier to the input conditions of a Nicolet Digital Storage Scope.

The time resolution of the photo diode and photomultiplier signals is such that the individual lasing spikes of the Nd glass laser are resolved.

Table 5. Tellurate Based Perovskites Prepared for Study.

Perovskite Tellurates

Perovskite Powders Prepared	Second Harmonic Generators (Piezoelectric)
Cd_2MnTeO_6	
Cd_2CaTeO_6	
Cd_2ZnTeO_6	
Cd_2CdTeO_6	
Cd_2MgTeO_6	Cd_2MgTeO_6
Sr_2MgTeO_6	
Sr_2MnTeO_6	
Sr_2SrTeO_6	Sr_2SrTeO_6
Sr_2CdTeO_6	Sr_2CdTeO_6
Sr_2CaTeO_6	Sr_2CaTeO_6
Sr_2ZnTeO_6	
Sr_2CoTeO_6	
Ca_2CoTeO_6	
Ca_2MgTeO_6	
Ca_2MnTeO_6	
Ca_2CaTeO_6	
Ca_2ZnTeO_6	
Ca_2CdTeO_6	

From the time correlation of driving and response functions, and the shape of the response pulses, it is easy to identify spurious signals which can result at higher power levels from excitation of a plasma at the crystalletic-gas interfaces.

Typical data taken upon a standard quartz powder is shown in Figure 18 By raising the gain in the multiplier system it can be shown that the system is capable of discerning harmonic signals from generators with less than 1/1000 th the signal level of quartz.

Figure 19a indicates the clear presence of an acentric phase in Sr_2CdTeO_6 and Figure 19b the complete absence of any harmonic signal from Cd_2CdTeO_6 under similar conditions of gain and excitation. For the tellurate phases which have been synthesized, Table 5 indicates that only four

Cd_2MgTeO_6

Sr_2SrTeO_6

Sr_2CdTeO_6

Sr_2CaTeO_6

are acentric at room temperature and thus of potential interest for further study in ceramic form or as additives to PZT formulations.

3.4.2. New 'Phases' for Piezoelectric Application

A new family of pyroniobates in the system $Sr_2Nb_2O_7:Ca_2Nb_2O_7$ have been synthesized by Nanamatsu et al. (13). Compositions in this field appear to be ferroelectric with Curie temperatures in the range 1375 to 1500°C which would make them the most stable known ferroelectrics.

It has been suggested (14, 15) that oxygen octahedron ferroelectrics which are uniaxial in macroscopic monocrystal form may be 'amorphized' or rendered partially amorphous to produce a three-dimensionally polarizable structure with "glass like" properties which may retain ferroelectric behavior. Prerequisites for materials which may be interesting are very strong ferroelectric coupling (high T_c) and a structure composed of three-dimensionally polarizable sub units (like the oxygen octahedron).

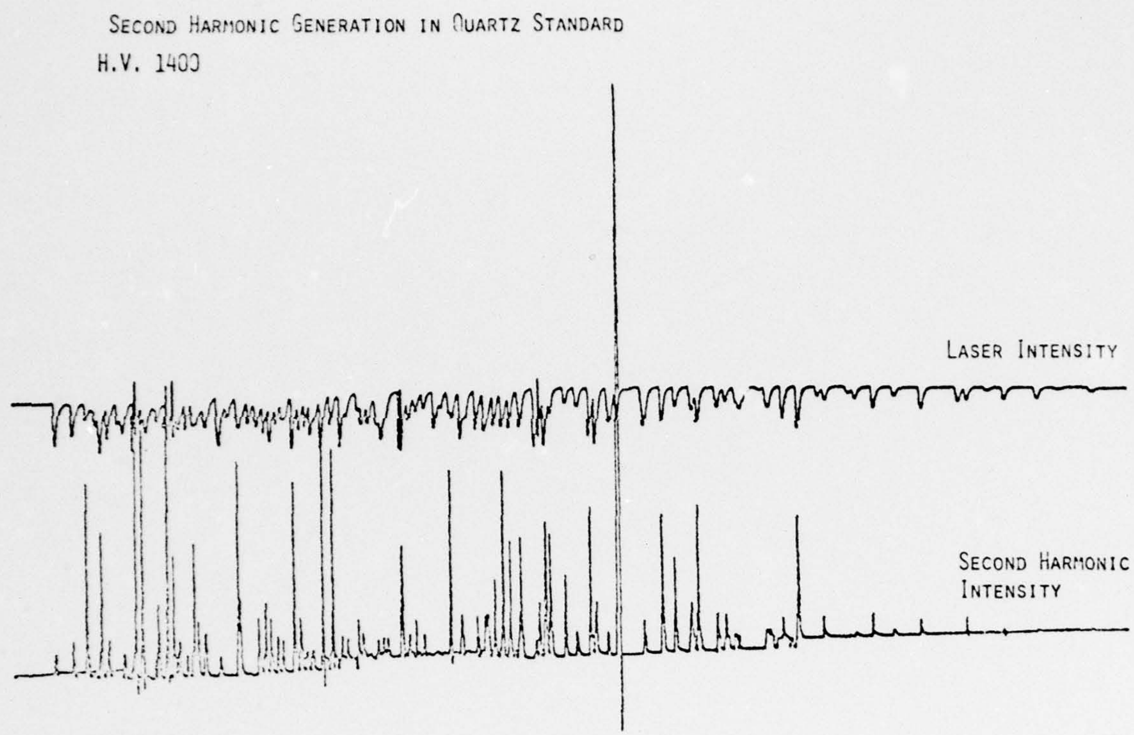

Fig. 18. S.H.G. response from standard Quartz powder.

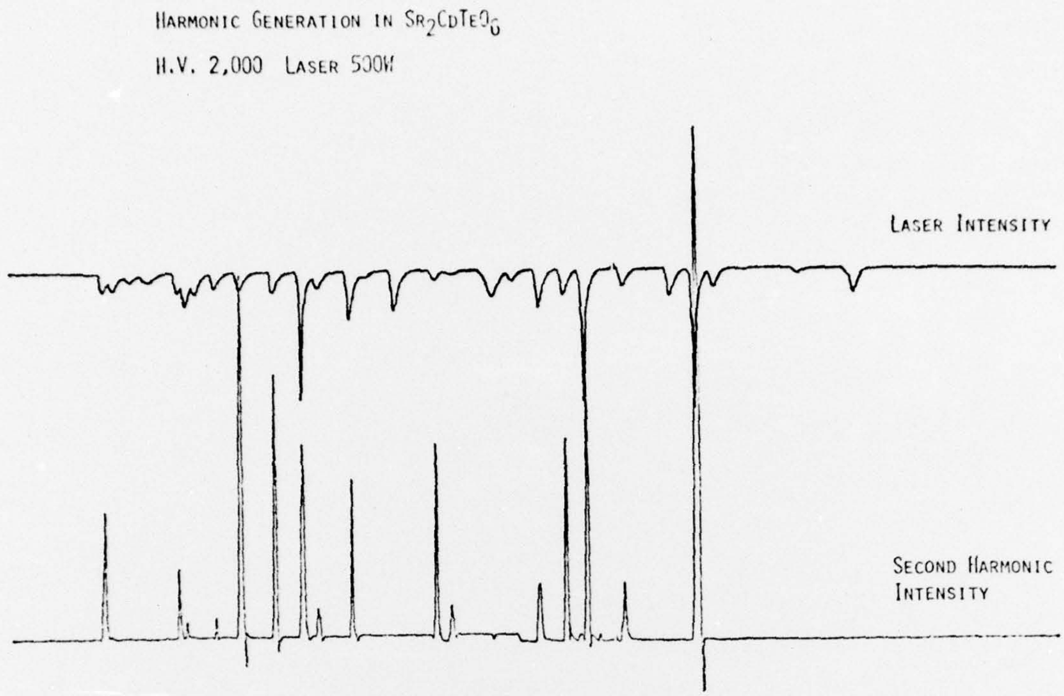

Fig. 19a. S.H.G. response in $Sr_2Cd_2TeO_6$ powder

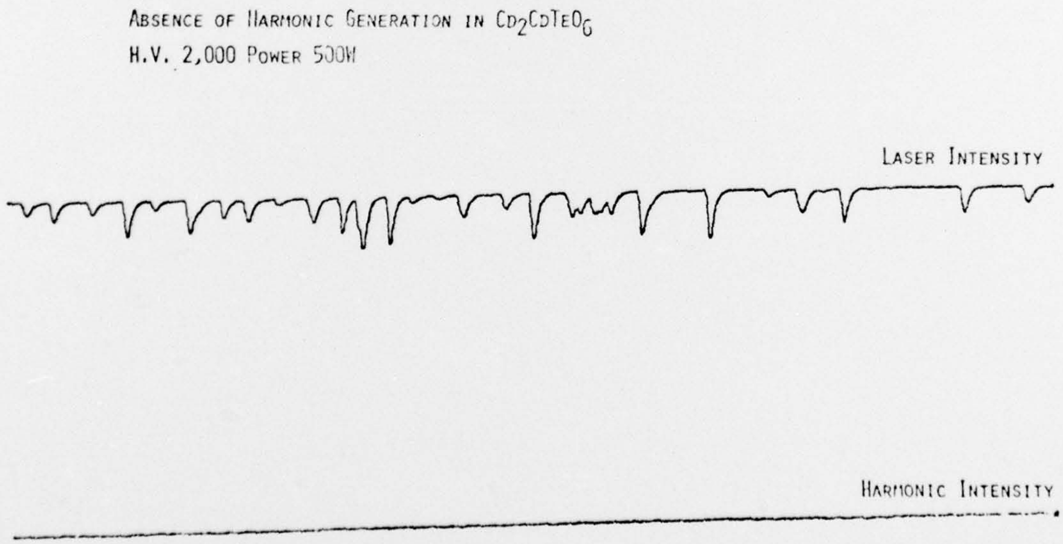

Fig. 19b. Absence of S.H.G. response in Cd_2CdTeO_6 under identical conditions to (a) above.

Studies by Nanamatsu have shown a highly distorted pyrochlore structure for the $Sr_2Nb_2O_7$ and in view of the very high T_c and possibility for strong piezoelectricity it was decided to study both amorphous and crystalline phases.

Powder and sintered ceramic samples of $Sr_2Nb_2O_7$ have been synthesized from carbonates and mixed oxides. The very refractory nature of the powder makes it difficult to sinter highly dense ceramics with present furnace equipment and a small gas fired high temperature kiln is being installed. Samples with 0.85 theoretical density have been made, and preliminary dielectric data shows a very low loss, high resistivity dielectric, however, connected porosity has so far frustrated attempts to pole the ceramic.

A program to sputter thin films of $Sr_2Nb_2O_7$ has been initiated, and very high quality, clear transparent films have been fabricated by A.C. sputtering either in argon, argon:oxygen or in oxygen carrier gas. Initial dielectric studies show that pinhole free capacitors can be readily fabricated on the sputtered films and dielectric measurements are now in progress to characterize the permittivity, loss tangent, and dispersion over the range 10 Hz to 50 MHz.

Initial films have been laid down upon room temperature recrystallized alumina substrates, upon platinum on alumina, and upon aluminum on alumina. Work is being initiated to study the influence of higher temperature annealing upon the dielectric response of the present films, and to study the influence of substrate temperature during the sputtering process.

A smaller subsidiary effort has been initiated to explore the highly refractory pyrochlore and distorted pyrochlore structure compounds in the rare earth metal titanate and stannate families. These are compounds in the system

$$Re_2Ti_2O_7:Re_2Sn_2O_7$$

where Re is a suitably chosen rare earth or lanthanum ion e.g., Nd, Gd, Tb,...

There is some evidence that the rare earth titanates are strongly polar, highly distorted pyrochlore derivative structures, whilst the stannates are cubic pyrochlores. If solid solution is possible between titanate and stannate end members, these ceramics could have bery interesting high temperature dielectric and piezoelectric properties.

3.5. Deliberately Inhomogeneous Ceramics

3.5.1. Control of the Elastic Boundary Conditions

PLZT has been chosen as the model system in which to explore the possibility of controlling the elastic boundary conditions by deliberately introducing a lamellar heterogeneity. Present work is concerned with:

(1) Evaluation of the thermal expansion anomalies associated with rhombohedral I:rhombohedral II phase change, and with the change from rhombohedral ferroelectric to orthorhombic antiferroelectric phase. Also, the normal thermal expansions in the higher temperature cubic phase are being measured. This data is absolutely necessary to design composition systems for the generation of particular stress distributions.

(2) Studies of the fabrication of doctor bladed multilayer PLZT structures, to ascertain the range of compositions which can be co-fired without delamination and to examine methods for implanting electrodes for poling.

3.5.2. Electrical Boundary Control

Work has been initiated to explore a number of compositions in the $PbTiO_3$:$PbZrO_3$:$PbSnO_3$:La_2O_3 system which exhibit suitable field forced antiferroelectric:ferroelectric phase transitions. Conventional pressed and sintered slugs are being fabricated to test switching parameters, and preliminary doctor blading studies have been initiated with the more suitable compositions.

3.5.3. Replamineform Transducers

Heretofore, efforts to generate two phase piezoelectric elements have not been singularly successful. A number of PZT:plastic combinations have been tried, but in every case the attenuation of the piezoelectric effect in the stiffer ceramic phase in penal.

We believe that this property degradation can be traced back to the mode of connectivity of the two phases. In the normal composite, low permittivity plastic layers interleave the ceramic grains preventing post forming poling, and attenuating the piezoelectric response.

Clearly the type of structure required for effective mixing is one in which both phases are three-dimensionally interconnected so that flux and stress paths are maintained between stressed and electroded surfaces.

During the last four years, an interesting method of forming a microstructure of just this type has been developed in MRL.

The process called replamineform uses a natural coral as an original 'template' for the structure. Since the coral polyp is a living organism, it must stay in contact with the sea water to survive. In growth, coral thus leaves a random network of channels for water penetration. The diameter of these near randomly interconnected 3-dimensional channels being determined by the coral species to suit its growth and nutrient sources vary from 10 to more than 100 μm. However, in any given species the channel diameter is remarkably uniform.

To reproduce the coral microstructural, a wax impregnation is made, the coral dissolved away in weak acid, then the coral phase is replaced by a suitable viscosity slip of the ceramic required.

Using the replamineform process, metal, plastic and ceramic replicas of a number of coral species have been fabricated and are now beginning to be used on an experimental basis in a range of biomedical applications.

For the transducer application, coral of the genus - species porites-porites has been used. The pores in this coral have a diameter of about 200 μm and occupy about 50% of the volume. A commercial PZT (Ultrasonics PZT-501) has been suspended in a water slurry and this suspension infused into a wax negative of the coral structure. Upon firing, the wax is slowly 'burned out' and a sintered PZT replica of the coral structure produced.

Early experimentation has been primarily concerned with optimizing the experimental technique for producing faithful replicas of the coral microstructure in relatively small samples. The best achieved to date is a robust 3 mm x 4 mm x 2.5 mm plate. This sample has been electroded and cycled on the Sawyer and Tower equipment. Values of P_R induced under fields $\sim$4 kv/cm agree well with P_R values for macroscopic disc samples indicating near perfect poling.

A sample poled under DC field of 4 kv/cm applied across the thin dimension was measured on the Berlincourt d_{33} meter also gave values which agree well with listed data for this composition.

Experiments are now being carried forward to evaluate aging, and the changes in poling, and aging associated with infusing polymers into the pore structure either before or after the poling operation.

3.6. Polar Ferroelastics

Optical and x-ray studies of the high temperature polar:polar phase change in $Ba_2GeTi_2O_8$ have shown conclusively that the original classification as Aizu species 4mmFmm2 is incorrect, and that the lower temperature point symmetry is either m or 1.

The four domain states corresponding to the ferroelastic point group m have been identified optically and ferroelastic switching between these states verified.

Current work is focused upon a more complete evaluation of the $Ba_2GeTi_2O_8$: $Ba_2SiTi_2O_8$ phase diagram, since a solid solution will certainly be required to bring the ferroelastic phase change in the germanate down into usable range. Unfortunately, it appears that single crystals are required to make any satisfactor assignment of the phase transition temperature.

We are cooperating with the crystal growth program under Dr. K. E. Spear at Penn State, who also requires these crystals for the evaluation of possible temperature compensated cuts.

3.7. Lithium Thallium Tartrate (LTT)

A small effort is being assigned to a study of the low temperature ferroelastic domain structure in LTT. Single crsytals cut in the form of 'a' plates are being examined under polarized monochromatic light. Examination of the preliminary measurements of the index ellipsoid suggest that sufficient domain contrast may occur due to the birefringence difference for a fitted 'a' axis orientation.

It has not yet been possible to take up the detailed structure refinement for LTT, as we have been unable to recruit a crystallography student who wishes to take up a refinement problem of this type.

4. EQUIPMENT AND ORGANIZATION

Over the first year of the contract a major effort has been required to put into service the new processing, fabrication and test equipment needed for the tasks proposed.

In this period, the following items of processing equipment have been installed, tested and are now in routine operation:

(1) Donaldson Acucut Particle Classifier, Model 12.

(2) Fluid Energy 4" Laboratory Micro-Jet Mill

(3) Astro Model 1000 High Temperature Furance

(4) Data-Trak Automatic Program Control

(5) Norton Ball Mill and Rack Assembly

(6) Carver Model 1259 Semi-automatic Pellet Press

The following additional major items are now in house and will be operational over the next six months:

(1) Stokes Model DD2 Automatic Rotary Table Press

(2) Hardtle Isostatic Gas Hot Pressing System

(3) Presco Model 251 Semi-automatic Printer

In test equipment, we have installed the complete Harrop thermal analysis system which includes:

(1) Model TG716 Thermogravimetric Analyzer

(2) Model DT716 Differential Thermal Analyzer

(3) Model TA700 Control Console

(4) Model TD716 Thermal Dilatometric Analyzer

New equipment for low temperature optical second harmonic light analysis:

(1) A Channel products d_{33} meter with d_{31} attachments

(2) Wide range automatic resonance analyzer

(3) Differential capacitance dilatometer

(4) High field Sawyer and Tower equipment with uniaxial stressing jig

Over the next few months we shall be installing new equipment for electrical pulse poling, additional optical equipment to initiate light scattering studies of domain wall motion in rhombohedral PLZTs and a new ultra-high sensitivity

capacitance dilatometer to look at dimensional creep during aging and deaging.

Organizationally we were delayed by a most unfortunate illness which greatly delayed, then finally frustrated the appointment of our original choice for senior postdoctoral fellow in the processing area. We were, however, fortunate to pick up the services of Dr. Leo Tarhay in the area of processing and characterization and efforts in this area are now back on schedule.

A most important part of the responsibility associated with a contract of this character which was both fundamental and applied aspects concerns the need to establish and maintain close working contact with a number of the major producers and users of piezoelectric materials and transducer systems.

Over the initial period, the following establishments have been visited for talks and consultation:

(1)	Naval Research Laboratory, Washington, D.C.	Paul Smith R. Pohanka
(2)	Naval Underwater Systems Command, New London, Connecticut	Charles LeBlanc M. Wollett
(3)	Linden Labs, Bellefonte, Pennsylvania	J. W. Anderson
(4)	Erie Technological Products, Erie, Pennsylvania	N. Coda
(5)	Honeywell, Inc., Minneapolis, Minnesota	R. Stokes J. Kyonka S. T. Liu
(6)	Itek Optical Systems, Lexington, Massachusetts	R. E. Aldrich
(7)	Lincoln Labs., Lexington, Massachusetts	D. Kocker

A good working relationship has been established with personnel in Linden Labs and the Erie Operations in State College.

Following a visit by Dr. J. V. Biggers and Dr. L. E. Cross to Honeywell Central Research Labs, arrangements were made for Dr. S. T. Liu to spend the month of December in the Materials Research Laboratory to study problems of mutual interest in piezoelectric and pyroelectric crystals.

Over the contract period, the following publications have been generated by senior personnel who are partially supported upon contract funds.

1. R. E. Newnham and L. E. Cross. Secondary Ferroics and Domain Divided Piezoelectrics. Ferroelectrics 10, 269-276 (1976).

2. L. E. Cross and T. W. Cline. Contribution to the Dielectric Response from Charged Domain Walls in $Pb_5Ge_3O_{11}$. Ferroelectrics 11, 333-336 (1976).

3. A. S. Bhalla and L. E. Cross. Growth of Some Ferroelectric Platinate and Stannate Single Crystals. J. Crystal Growth 31, 77 (1976).

4. R. E. Newnham. Phase Diagrams and Crystal Chemistry. Chapter in Phase Diagrams: Materials Science and Technology. Edited by A. M. Alper, Academic Press, New York (accepted).

5. R. E. Newnham. Articles on Magnetic Minerals and Jade. Encyclopedia of Earth Science (accepted).

6. R. E. Newnham and Doyle P. Skinner, Jr. Polycrystalline Secondary Ferroics. Mat. Res. Bull. 11, 1273 (1976).

*7. R. E. Newnham and L. E. Cross. Tailored Domains in Quartz and Other Piezoelectrics. Proc. 30th Annual Frequency Control Symp., U.S. Army Electronics Command, p. 71 (1976).

*8. W. A. Schulze, J. V. Biggers and L. E. Cross. Aging of Dielectric Dispersion in PLZT Relaxor Ceramics. J. Am. Ceram. Soc. (submitted).

*9. S. T. Liu and L. E. Cross. Primary Pyroelectricity in Strontium Barium Niobate. Phys. Stat. Sol. B (submitted).

*10. A. Bhalla and L. E. Cross. A Simple Technique for Decorating Ferroelectric Domains in Gadolinium Molybdate. J. Mats. Sci. (submitted).

11. J. L. Kirk, L. E. Cross and J. P. Dougherty. Pressure and Temperature Dependence of the Dielectric Properties and Phase Transitions in Ferroelectric $Pb_5Ge_3O_{11}$. Ferroelectrics 11, 439 (1976).

*Papers and talks with subject matter directly supported by ONR:DARPA funds.

REFERENCES

1. A. F. Devonshire, Phil. Mag., 40, 1040 (1949).

2. A. F. Devonshire, Phil. Mag., 42, 1065 (1951).

3. A. F. Devonshire, Phil. Mag. Suppl., 3, 85 (1954).

4. W. R. Buessem, L. E. Cross and A. K. Goswami, J. Am. Ceram. Soc., 49, 33 (1966).

5. W. R. Buessem, L. E. Cross and A. K. Goswami, J. Am. Ceram. Soc., 49, 36 (1966).

6. J. V. Biggers and W. Schulze, Sprague Electric Co. Reports, Annual Reports 1, 2, 3 (1973 to 1976).

7. W. R. Buessem and T. I. Prokopowicz, Ferroelectrics 10, 225 (1976).

8. W. A. Schulze and J. V. Biggers, Ferroelectrics 9, 203 (1975).

9. S. C. Abrahams, S. K. Kurtz and P. B. Jamieson, Phys. Rev., 172, 551 (1968).

10. See for example Landolt-Börnstein, Vol. III 3 and III 9, Ferroelectric and Antiferroelectric Substances.

11. E. D. Politova, Yu. N. Venevtsev, Dokl. Acad. Nauk SSSR 209, 838 (1973).

12. S. K. Kurtz and T. T. Perry, J. Appl. Phys., 39, 3798 (1969).

13. S. Nanamatsu, M. Kimura and T. Kawamura, J. Phys. Soc. Japan 38, 817 (1975).

14. A. M. Glass, K. Nassau and J. W. Schiver, Annual Meeting Materials Research Society, Boston, Mass., November 15-17, 1976.

15. M. E. Lines, Annual Meeting Materials Research Society, Boston, Mass., November 15-17, 1976.

Unclassified

SECURITY CLASSIFICATION OF THIS PAGE (When Data Entered)

REPORT DOCUMENTATION PAGE		READ INSTRUCTIONS BEFORE COMPLETING FORM
1. REPORT NUMBER	2. GOVT ACCESSION NO.	3. RECIPIENT'S CATALOG NUMBER
4. TITLE (and Subtitle) 6 Ceramic Piezoelectric Transducers.		5. TYPE OF REPORT & PERIOD COVERED Annual Report January 1 - December 31, 1976
		6. PERFORMING ORG. REPORT NUMBER
7. AUTHOR(s) 10 L.E. Cross, J.V. Biggers and R.E. Newnham		8. CONTRACT OR GRANT NUMBER(s) 15 N00014-76-C-0515 new
9. PERFORMING ORGANIZATION NAME AND ADDRESS Materials Research Laboratory, The Pennsylvania State University, University Park, PA 16802		10. PROGRAM ELEMENT, PROJECT, TASK AREA & WORK UNIT NUMBERS
11. CONTROLLING OFFICE NAME AND ADDRESS Office of Naval Research, Ballston Tower, Arlington, VA 22217		12. REPORT DATE 11 31 January 31, 1977
		13. NUMBER OF PAGES 65
14. MONITORING AGENCY NAME & ADDRESS (if different from Controlling Office) Dr. A. M. Diness, Room 619, Ballston Towers, 800 N. Quincy Street, Arlington, VA 22217 12 67p.		15. SECURITY CLASS. (of this report) Unclassified
		15a. DECLASSIFICATION/DOWNGRADING SCHEDULE -

16. DISTRIBUTION STATEMENT (of this Report)

9 Annual summary rept. 1 Jan - 31 Dec 76

Approved for Public Release; Distribution Unlimited

17. DISTRIBUTION STATEMENT (of the abstract entered in Block 20, if different from Report)

18. SUPPLEMENTARY NOTES

19. KEY WORDS (Continue on reverse side if necessary and identify by block number)

Piezoelectric, Ceramic, Transducer, Ferroelectric, Electrostrictive, Dielectric

20. ABSTRACT (Continue on reverse side if necessary and identify by block number)

This report documents progress in the first year of a comprehensive program to develop new and improved materials for ceramic piezoelectric transducers. For many years, formulations in the $PbZrO_3$:$PbTiO_3$ (PZT) family of ferroelectric solid solutions, with compositions chosen to be close to the morphotropic rhombohedral:tetragonal ferroelectric phase transition have been widely used for transducers.

For these conventional PZT type ceramics this program seeks to clarify the roles of the different deformation mechanisms in both 'hard' and 'soft' formula-

DD FORM 1 JAN 73 1473 EDITION OF 1 NOV 65 IS OBSOLETE

S/N 0102-014-6601

Unclassified

SECURITY CLASSIFICATION OF THIS PAGE (When Data Entered)

220 750

4B

tions, and to clearly delineate the influence of the ceramic microstructure in modifying the 'averaged' single crystal properties of the constituent crystallites.

These studies include a careful intercomparison of the microstructure, chemical microhomogeneity and physical properties of samples with precisely controlled initial chemistry, fabricated by a wide range of different ceramic techniques. To aid in the separation of single crystal 'single domain' properties, a phenomenological Elastic Gibbs function to describe PZTs with compositions close to the morphotropic boundary is being developed, and ADAGE computer graphic methods are being developed to depict the full three-dimensional polarization surfaces near the stable phases so that the role of internal stresses and electric fields can be quantitatively analyzed.

To attempt more radical advance in polycrystal materials three different approaches are being taken:

(1) To broaden the composition base for transducers fabricated by traditional methods, we seek new ferroelectric compounds with high Curie temperature and high effective prototypic symmetry. Tellurium containing compounds with perovskite structure in the family Sr_2CdTeO_6 which have been reported to have ferroic transition temperatures up to 960°C are being studied. In the less symmetric $Sr_2Nb_2O_7$ and $Nd_2Ti_2O_7$ pyrochlore derivative structures very high Curie temperature up to 1650°C have been reported. Techniques are being developed to produce glass or microcrystalline materials in these families, seeking "glass-like" ferroelectric properties and materials which would be polable in any orientation.

(2) To break the original boundary condition of macroscopic homogeneity deliberate composition gradients are being introduced by co-firing stacked layers of tape cast thin sections with suitably controlled composition. Preliminary studies show that both ferroelectric and antiferroelectric formulations can be co-fired, promising a range of control of both electrical poling and elastic stress distribution in these structures.

(3) To eliminate the need for exceedingly high prototype symmetry, grain oriented ceramics are being developed as a potential "hybrid" between single crystal and ceramic forms. Initial work is concentrated on the family of bismuth oxide layer structure ferroelectrics where the platy morphology of the micro-crystals allows the use of many simple ceramic techniques for generating oriented microstructures.

A new type of device is under study which makes the use of a multilayer monolithic structure with integrated electrodes to generate large electrostrictive deformations at low applied voltages in an unpoled high K dielectric. These elements show considerable promise for displacement transducers in adaptive optics and as controllable generators for acoustic holography.